

Copyright Warning & Restrictions

The copyright law of the United States (Title 17, United States Code) governs the making of photocopies or other reproductions of copyrighted material.

Under certain conditions specified in the law, libraries and archives are authorized to furnish a photocopy or other reproduction. One of these specified conditions is that the photocopy or reproduction is not to be “used for any purpose other than private study, scholarship, or research.” If a user makes a request for, or later uses, a photocopy or reproduction for purposes in excess of “fair use” that user may be liable for copyright infringement,

This institution reserves the right to refuse to accept a copying order if, in its judgment, fulfillment of the order would involve violation of copyright law.

Please Note: The author retains the copyright while the New Jersey Institute of Technology reserves the right to distribute this thesis or dissertation

Printing note: If you do not wish to print this page, then select “Pages from: first page # to: last page #” on the print dialog screen

The Van Houten library has removed some of the personal information and all signatures from the approval page and biographical sketches of theses and dissertations in order to protect the identity of NJIT graduates and faculty.

ABSTRACT

CORRELATION BETWEEN TIDAL VOLUME MEASURED BY SPIROMETRY AND IMPEDANCE PNEUMOGRAPHY

by
Krithika Seshadri

In this study, an alternative method, impedance pneumography was used to measure the respiration volume. The respiration volume was measured both by using a conventional spirometer and an impedance pneumograph, and evaluated quantitatively in 17 subjects using linear and nonlinear regression algorithms.

Data were collected from 17 normal, healthy subjects during rest and paced breathing conditions. A technique was developed to measure tidal volume by impedance pneumography. The respiration volume measured by the spirometer was correlated with the volume measured by the pneumograph. Different electrode positions and postures were included in the study to determine the position and posture which would yield optimum correlations.

Correlations between the tidal volume measured by the spirometer and the tidal volume measured by the pneumograph, the rates of respiration (exhalation and inhalation widths), and the means and standard deviations of the exhalation ranges were computed. Results showed high correlations between the two techniques used. The position of the electrodes played a major role in affecting correlations. It was concluded that the posterior electrode position yielded relatively high correlations for the seated and standing postures and that the lateral position yielded good correlations for the supine posture, but further exploration is necessary to determine other factors which would influence the results.

**CORRELATION BETWEEN TIDAL VOLUME MEASURED BY SPIROMETRY
AND IMPEDANCE PNEUMOGRAPHY**

by
Krithika Seshadri

A Thesis
Submitted to the Faculty of
New Jersey Institute of Technology
in Partial Fulfillment of the Requirements for the Degree
Master of Science in Biomedical Engineering

Biomedical Engineering Committee

October 1994

APPROVAL PAGE

**CORRELATION BETWEEN TIDAL VOLUME MEASURED BY SPIROMETRY
AND IMPEDANCE PNEUMOGRAPHY**

Krithika Seshadri

Dr. Stanley Reisman, Thesis Adviser Date
Professor of Electrical Engineering and Biomedical Engineering, NJIT, NJ

Dr. David Kristol, Committee Member Date
Director of Biomedical Engineering program, NJIT, NJ

Dr. Thomas Findley, Committee Member Date
Director of Research, Kessler Institute for Rehabilitation, West Orange, NJ

Blank Page

BIOGRAPHICAL SKETCH

Author: Krithika Seshadri

Degree: Master of Science in Biomedical Engineering

Date: October 1994

Undergraduate and Graduate Education:

- Master of Science in Biomedical Engineering
New Jersey Institute of Technology, Newark, NJ, 1994
- Bachelor of Science in Engineering
Sri Jayachamarajendra College of Engineering, Mysore, India, 1991

Major: Biomedical Engineering

Presentations and Publications:

K. Seshadri, S. Reisman, M. Daum, R. Zorowitz, and R. DeMeersman, "Heart Rate Variability in Stroke Population and Normals: A Comparison using Spectral Analysis". 20th Annual Northeast Bioengineering Conference. Springfield, Massachusetts, 17-18 March 1994.

This Thesis is dedicated to
my loving husband Suresh Sundararaman, who encouraged and helped me accomplish
this, my parents Sathy & Seshadri, my brother Kannan, my grandmother Ponnamma
Swamy and Rattu who always believed in me.

ACKNOWLEDGMENT

The author wishes to express her sincere gratitude to her adviser, Dr. Stanley Reisman for his guidance, moral support and encouragement without which this research would have been impossible.

Special thanks to Dr. Ronald DeMeersman and Ms. Miriam Daum, who took time out of their busy schedules to answer the author's physiology-related questions. The author is thankful to Dr. David Kristol, for having given her an opportunity to continue her education.

The author is particularly grateful to Dr. Thomas Findley and Kessler Institute for Rehabilitation for providing a stimulating and intellectual environment that encourages research. The author's sincere thanks to Ms. Melissa Leifer who helped the author learn the system at Kessler. The author is indebted to John Andrews for his help.

Finally, the author extends her appreciation to all the subjects who sacrificed their comfort for the advancement of science and all others who have helped during the course of this project.

TABLE OF CONTENTS

Chapter	Page
1 BACKGROUND	
1.1 Introduction	1
1.2 Purpose of project	1
1.3 Cardiovascular Physiology	2
1.4 The Heart-Anatomy.....	5
1.5 Respiratory system-Organization	6
1.6 Ventilation and Lung Mechanics	10
1.7 Lung volumes.....	18
1.8 Impedance Pneumography.....	19
1.9 Prior research	23
2 METHODS	
2.1 Methods	28
2.2 Data Acquisition	32
2.3 Signal processing	35
2.4 Data analysis	37
3 RESULTS	
3.1 Frequency response of the impedance pneumograph	42
3.2 Lead II electrode configuration results	47
3.3 Linear regression results	48
3.4 Nonlinear modeling	51
4 DISCUSSION AND CONCLUSIONS	
4.1 Discussion	60
4.2 Conclusions	66
4.3 Suggestions for future research	67

Chapter	Page
APPENDIX 1 Data acquisition	73
APPENDIX 2 Correlation	74
APPENDIX 3 S-Plus programs	75
APPENDIX 4 Matlab filter design	84
APPENDIX 5 S-Plus functions	85
APPENDIX 6 Tables	95
REFERENCES	106

LIST OF TABLES

Table	Page
3.1 Correlation coefficients for the lead II electrode configuration	47
3.2 Linear regression results for subject #1	50
3.3 Linear regression results for subject #2	96
3.4 Linear regression results for subject #3	97
3.5 Linear regression results for subject #4	98
3.6 Linear regression results for subject #5	99
3.7 Linear regression results for subject #6	100
3.8 Results of the GAM using 3 transform functions and 2 predictors	54
3.9 Improved results of the GAM using 3 transform functions and 5 predictors.....	55
3.10 Nonlinear regression results for subject #1	59
3.11 Nonlinear regression results for subject #2	101
3.12 Nonlinear regression results for subject #3	102
3.13 Nonlinear regression results for subject #4	103
3.14 Nonlinear regression results for subject #5	104
3.15 Nonlinear regression results for subject #6.....	105

LIST OF FIGURES

Figure	Page
1.1 Circulation.....	3
1.2 The heart.....	4
1.3 Diagrammatic section of the heart.....	6
1.4 Respiratory system organization.....	7
1.5 Fick's law of diffusion.....	8
1.6 Airway branching.....	10
1.7 Steps of respiration.....	12
1.8 Muscles of respiration.....	13
1.9 Intercostal muscles.....	14
1.10 Pressure-Volume curve of an excised lung.....	15
1.11 Surface tension.....	16
1.12 Measurement of regional differences using radioactive xenon.....	16
1.13 Effects of compliance and airway resistance.....	17
1.14 Simple representation of the lungs.....	18
1.15 Spirometer recording of lung volumes and capacities	19
1.16 Impedance pneumograph	22
1.17 Amplitude modulation	22
1.18 Impedance changes versus electrode positions in man	24
2.1 Different electrode positions used in the study.....	30
2.2 Typical respiration signal acquired from the pneumograph.....	33

Figure	Page
2.3 Spirometer recording of tidal volume	34
2.4 Superimposed spirometer and pneumograph signals	35
2.5 Superimposed spirometer and smoothed respiration signals	36
2.6 Flowchart for obtaining the positions of exhalation and inhalation widths	38
2.7 Flowchart for obtaining the respiratory volume from the pneumograph.....	39
2.8 Flowchart for obtaining the tidal volume from the spirometer.....	40
2.9 Flowchart for obtaining the mean and standard deviation of exhalation widths.....	41
3.1 Response of the Resp 1	42
3.2 Typical first order system response	43
3.3 Simulated inputs for pacing at 8, 12, and 18 bpm and corresponding filter outputs.	44
3.4 Unit step input and the corresponding filter output	45
3.5 Transfer function of a system in time and frequency domains	46
3.6 Individual contributions of the 5 predictors for the example in table 3.9, using the "lo" transform function	55
4.1 A schematic representation of probable pathway of the current across thorax wall during deflated and inflated conditions in a dog	65
4.2 Mechanisms of airway obstruction	69
4.3 Bronchial wall in a normal and an asthmatic	70
4.4 Forces exerted on airway wall by the surrounding parenchyma in normal condition, emphysema and fibrosis	71

CHAPTER 1

BACKGROUND

1.1 Introduction

Breathing patterns and the related circulatory fluctuations may reflect the action of regulatory mechanisms and the lung mechanics on circulation. The study of such patterns and their correlations to other physiological parameters can enhance our knowledge of these mechanisms, both in normal and pathological conditions. This paper provides insight into the relationship between the breath-to-breath volume and the chest movements - inspiration and expiration. The main focus of this chapter is to provide adequate physiological background.

1.2 Purpose of project

This project is part of the ongoing research at the Kessler Institute for Rehabilitation. The overall objective of the research is to determine parasympathetic function as measured by heart rate variability (HRV) in patients over a one-year period following stroke. This is accomplished by performing spectral analysis on the processed electrocardiogram (EKG), respiration, blood pressure and metabolic data. The laboratory is comprised of instrumentation capable of collecting EKG, respiration, blood pressure, metabolic data and equipment to perform data analysis.

The results obtained from HRV studies are used for clinical purposes to predict adverse cardiac events. The author's project is part of the HRV project. The goal of this project is to find an alternative method for measuring tidal volume, that is, to find the correlation between tidal volume measured using two instruments- the spirometer and the impedance pneumograph. If good correlation is found to exist, the volume can then be measured using impedance pneumography (since the same instrumentation is also used to

record EKG) and the spirometer can be eliminated from the study. The main objective of the author's project is to correlate (Appendix 2) the volume at every breath as measured by the spirometer (an instrument used for measuring lung volumes) and as measured by an impedance pneumograph (see section 1.8 for a discussion of impedance pneumography). Part of the protocol used for HRV studies is used for the author's study (Chapter 2). The volume at each breath (tidal volume) is measured using a spirometer and the respiratory volume at each breath is measured by impedance pneumography.

1.3 Cardiovascular physiology

Cardiovascular physiology as an experimental science began in 1628, when the British physiologist William Harvey demonstrated that the cardiovascular system forms a circle, so that blood pumped out of the heart through one set of vessels, returns to the heart via a different set. There are actually two circuits (Figure 1.1), both originating and terminating in the heart, which is divided longitudinally into two functional halves[51]. Each half contains two chambers: an atrium and a ventricle (Figure1.2). The atrium on each side empties into the ventricle on that side, but there is no direct communication between the two atria or the two ventricles.

Blood is pumped via one circuit (the pulmonary circulation) from the right ventricle through the lungs and back to the heart via the left atrium. It is pumped via the other circuit (the systemic circulation) from the left ventricle through all the tissues of the body except the lungs and back into the heart via the right atrium. In both circuits, the vessels carrying blood away from the heart are called arteries and those carrying blood from the lungs or all other parts of the body (peripheral organs and tissues) back to the heart are called veins.

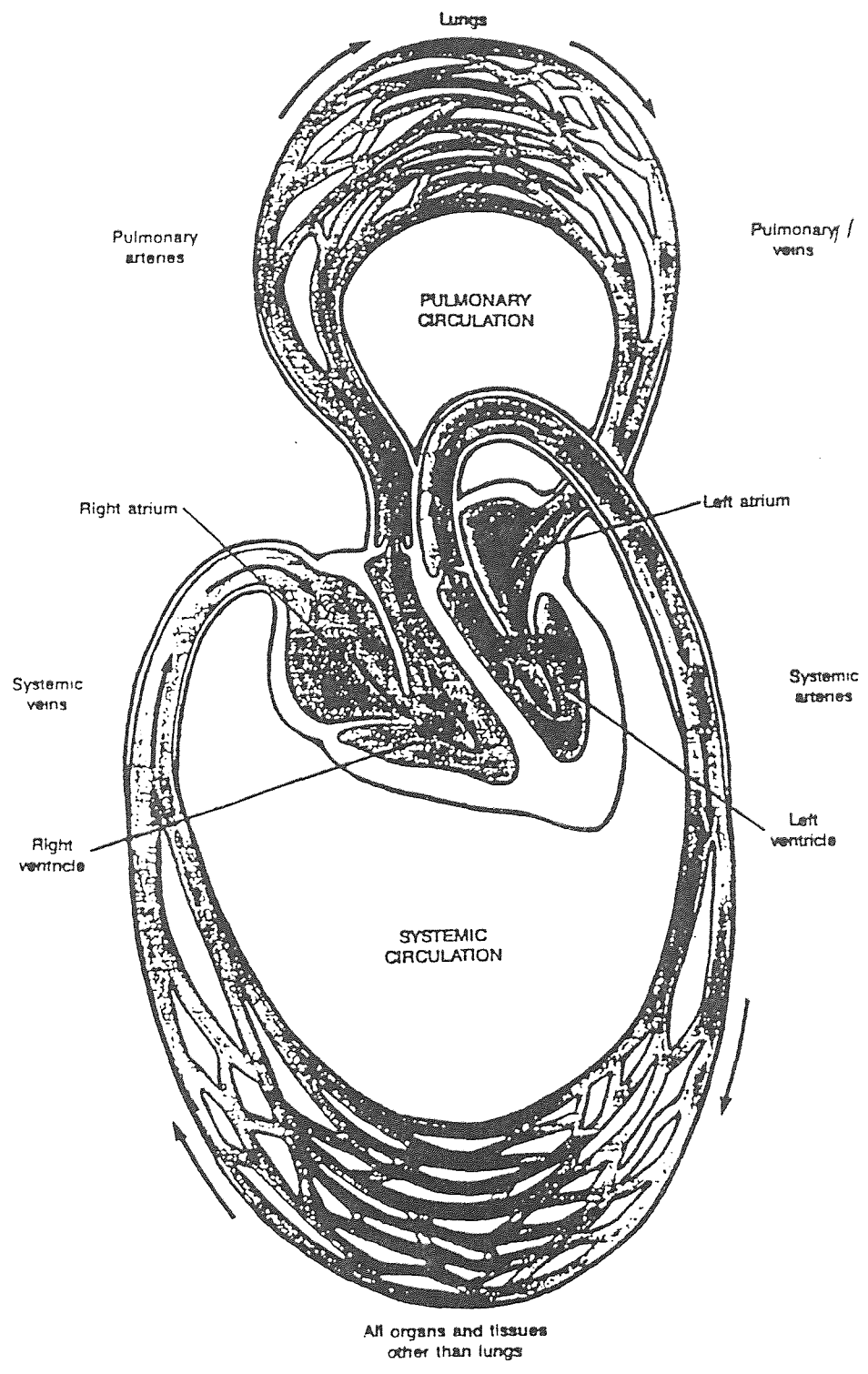


Figure 1.1 Circulation

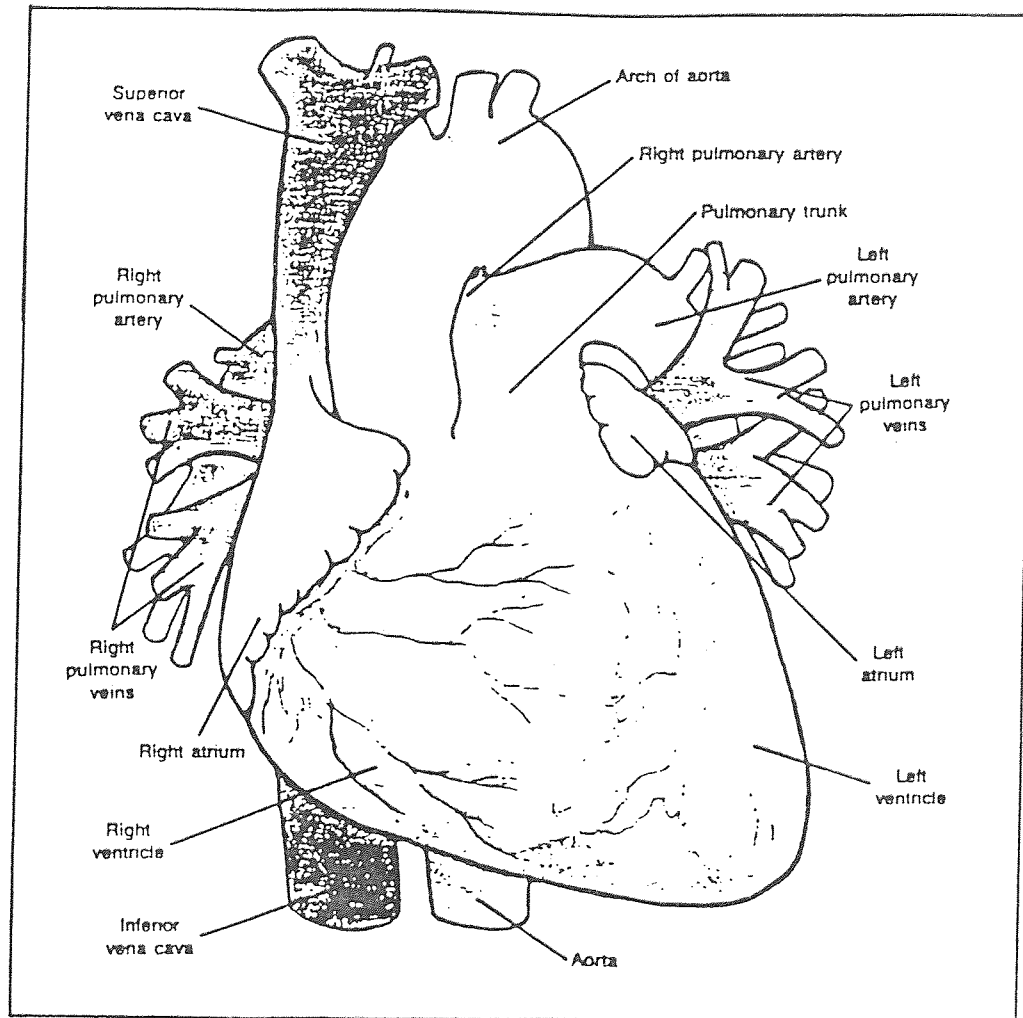


Figure 1.2 The heart

In the systemic circuit, blood leaves the left ventricle via a single large artery, the aorta (Figure 1.2). The systemic arteries branch from the aorta, dividing into progressively smaller branches. The smallest arteries form arterioles that branch into a huge number of very small, one-cell-thick vessels, the capillaries, which unite to form larger and thicker vessels, the venules. The arterioles, capillaries and the venules are collectively termed the micro circulation.

The venules in the systemic circulation then unite to form larger vessels, the veins. The veins from the peripheral organs and tissues unite to produce two large veins, the inferior vena cava, which collects blood from the lower portion of the body, and the superior vena cava, from the upper half of the body. It is through these two veins that blood is returned to the right atrium.

The pulmonary circulation is composed of a similar circuit. Blood leaves the right ventricle via a single large artery, the pulmonary trunk, which divides into the two pulmonary arteries, one supplying each lung. In the lungs, the arteries continue to branch, ultimately forming capillaries that unite into venules and then veins. The blood leaves the lungs via four pulmonary veins, which empty into the left atrium.

Blood can pass from the systemic veins to the systemic arteries only by first being pumped through the lungs. Thus, all the blood returning from the body's peripheral organs and tissues via the systemic veins is oxygenated before it is pumped back to them.

The lungs receive all the blood pumped by the right heart, whereas each of the peripheral organs and tissues receives only a fraction of the blood pumped by the left ventricle [51].

1.4 The Heart - Anatomy

The heart is a muscular organ enclosed in a fibrous sac, the pericardium, and located in the chest (thorax). The narrow space between the pericardium and the heart is filled with a watery fluid that serves as a lubricant as the heart moves within the sac.

The walls of the heart are composed primarily of cardiac muscle cells and are termed the myocardium[51]. The inner surface of the myocardium, that is, the surface in contact with the blood within the cardiac chambers, is lined by a thin layer of cells known as endothelial cells or endothelium. The endothelial cells line the entire vascular system .

Located between the atrium and ventricle in each half of the heart are the atrioventricular valves (AV valves), which permit blood to flow from atrium to ventricle

(Figure 1.3). The right AV valve is called the tricuspid valve and the left, the mitral valve. The opening and the closing of the AV valves is a passive process resulting from pressure differences across the valves.

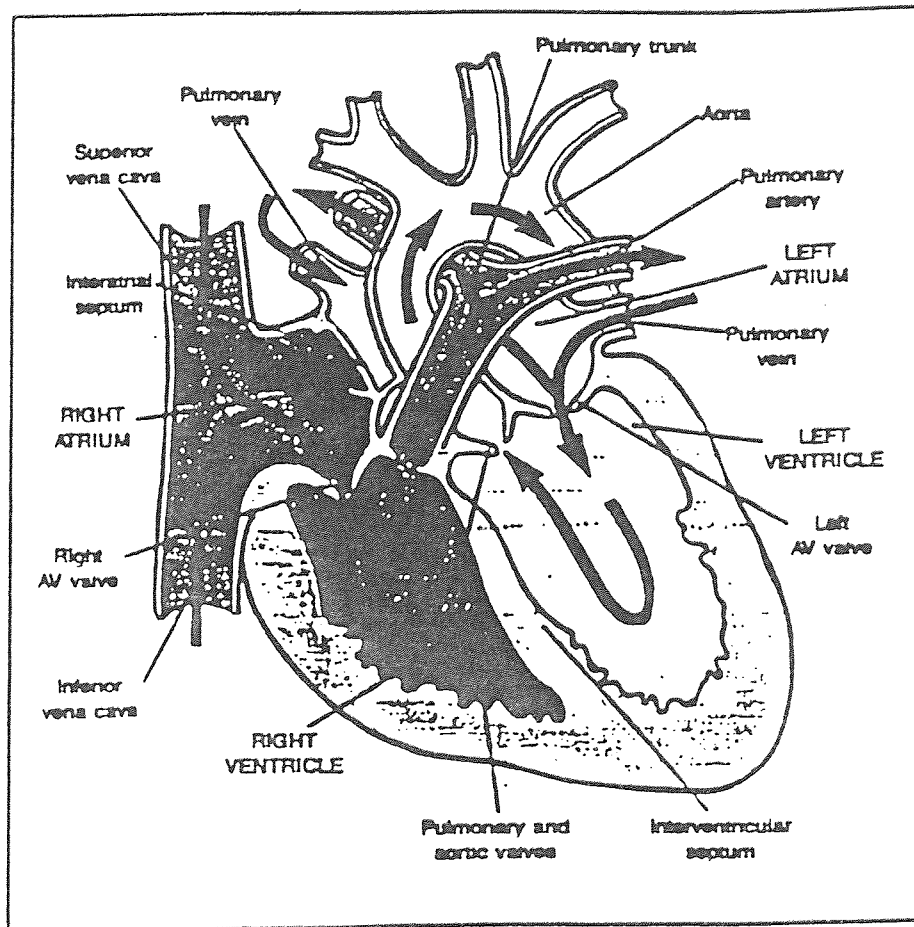


Figure 1.3 Diagrammatic section of the heart

1.5 Respiratory system - Organization

Respiration is defined as the exchange of oxygen (O_2) and carbon dioxide (CO_2) between an organism and the external environment.

There are two lungs, the right and the left, each divided into several lobes (Figure 1.4). The lungs consist mainly of tiny air-containing sacs called alveoli which are the sites of gas exchange with the blood. The airways are all the tubes through which air flows between the external environment and the alveoli.

Inspiration is the movement of air from the external environment through the airways into the alveoli during breathing. Expiration is movement in the opposite direction. An inspiration and an expiration constitute a respiratory cycle. During the entire cycle, the right ventricle of the heart continuously pumps blood through the capillaries surrounding each alveolus. At rest, in a normal adult, approximately 4 liters of environmental air enters and leaves the alveoli per minute while 5 liters of blood, the entire cardiac output, flows through the pulmonary capillaries. During heavy exercise, the air flow can increase 30-40 fold and the blood flow, 5-6 fold. The alveolar air and the capillary blood are separated from each other by an extremely thin membrane across which O_2 can diffuse [55].

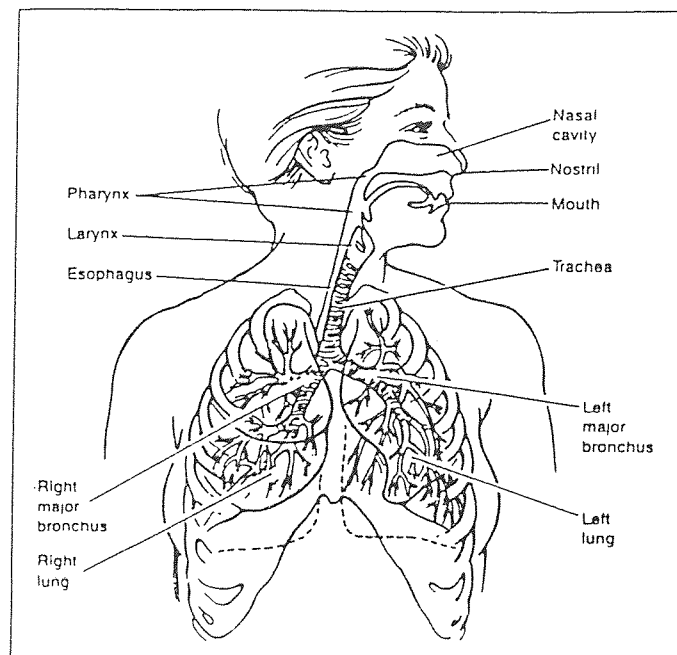


Figure 1.4 Respiratory system organization

The main function of the lung is for gas exchange. Its cardinal function is to allow oxygen to move from the air into the venous blood and for carbon dioxide to move from the venous blood to the air. It also acts as a reservoir for blood. Oxygen and carbon dioxide move between air inside the lungs and blood by simple diffusion, that is, from an area of high partial pressure to an area of low partial pressure. This is explained using Fick's law of diffusion. The law states that[53] the rate of transfer of a gas through a sheet of tissue is proportional to the tissue area (A) and the difference in gas partial pressure (P1-P2) between the two sides, and inversely proportional to the tissue thickness (T). (Figure 1.5).

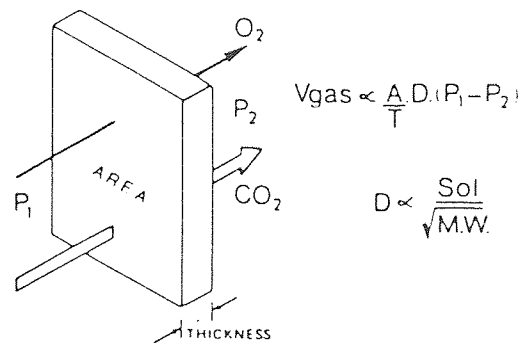


Figure 1.5 Fick's law of diffusion

$$V_{\text{gas}} \propto AD(P_1 - P_2) / T \quad (1.1)$$

where D is the diffusion constant. D is proportional to the gas solubility (Sol), but inversely proportional to the square root of its molecular weight (MW) as given by the equation

$$D \propto \text{Sol} / \sqrt{\text{MW}} \quad (1.2)$$

The lung generates a large diffusion area by being divided into myriads of units. Air is brought to one side of the blood-gas interface by airways and blood to the other side by blood vessels.

The airways of the lungs consist of a series of branching tubes which become narrower, shorter, and more numerous as they penetrate deeper into the lung[51]. The trachea divides into right and left main bronchi, which in turn divide into the lobar, then segmental bronchi (Figure 1.6). This process continues down to the terminal bronchioles, which are the smallest airways without alveoli. All these bronchi make up the conducting zone, whose function is to lead inspired air to the gas exchanging regions of the lung.

The terminal bronchioles divide into respiratory bronchioles, which have some alveoli budding from their walls. The alveolar ducts are the final parts which are completely lined with alveoli. This is the region of the lung where the gas exchange occurs and it is called the respiratory zone, and makes up most of the lung.

During inspiration, air passes into the pharynx which branches into the esophagus and the larynx (Figure 1.4), which houses the vocal chords. The larynx opens into a long tube, the trachea, which in turn branches into two bronchi, one of which enters each lung. The airway branching is summarized in Figure 1.6.

The lungs, like the heart, are situated in the thorax, the compartment of the body between the neck and the abdomen. The thorax is a closed compartment, bounded at the neck by muscles and connective tissue and completely separated from the abdomen by a large dome-shaped sheet of skeletal muscle, the diaphragm. The wall of the thorax is formed by the spinal column, the ribs, the breastbone (sternum), and the intercostal muscles. Each lung is surrounded by a completely closed sac, called the pleural sac consisting of thin sheets of cells called pleura, which are separated by an extremely thin layer of intrapleural fluid.

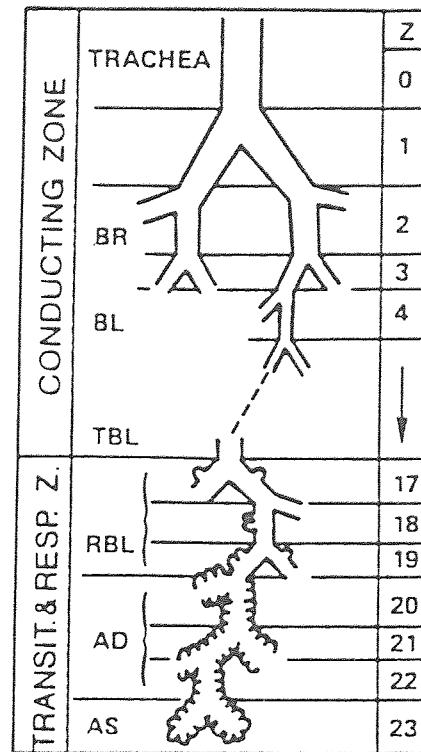


Figure 1.6 Airway branching

Both the lungs and the thoracic wall are elastic in nature. The volume of the lungs and the thorax at the end of a relaxed expiration is determined by passive elastic forces. All pressures in the respiratory system are relative to atmospheric pressure. The pressure within the lungs is called the alveolar pressure, the pressure in the intrapleural fluid is called the intrapleural pressure and the pressure difference across the lung wall is called the transpulmonary pressure, which holds the lungs open i.e., prevents them from collapsing.

1.6 Ventilation and Lung mechanics

Ventilation is defined as the exchange of air between the atmosphere and alveoli[51]. Like blood, air moves by bulk flow from a region of higher pressure to one of lower pressure. Bulk flow is described by the equation

$$F = \Delta P / R \quad (1.3)$$

where F = flow, P = pressure and R = resistance.

Equation (1.3) states that the flow is proportional to the pressure difference between two points and inversely proportional to the resistance. For the flow of air into or out of the lungs, the important pressures are the atmospheric pressure (P_{atm}) and the alveolar pressure (P_{alv}). Equation (1.3) then becomes

$$F = (P_{alv} - P_{int}) / R \quad (1.4)$$

Air moves into and out of the lungs because the alveolar pressure is made alternately lesser and greater than the atmospheric pressure[55]. The pressure changes are caused by changes in lung dimensions. Boyle's law helps to understand the relationship between pressure and volume. It is given by the equation

$$PV = \beta \text{ (at constant temperature)} \quad (1.5)$$

where β = a constant, P = pressure and V = volume. The law states that the relationship between the pressure exerted by a fixed number of gas molecules in a container and the volume of the container is as follows: An increase in the volume of the container decreases the pressure of the gas, whereas a decrease in volume increases the pressure.

The steps involved in respiration are shown in Figure 1.7. Initially, ventilation takes place by bulk flow followed by exchange by diffusion of oxygen and carbon dioxide between alveolar air and blood in lung capillaries. This is then followed by transport of gases through pulmonary and systemic circulations. Then, the exchange of

gases between blood in the tissue capillaries and cells in tissues takes place by diffusion and finally, cellular utilization of oxygen and production of carbon dioxide takes place.

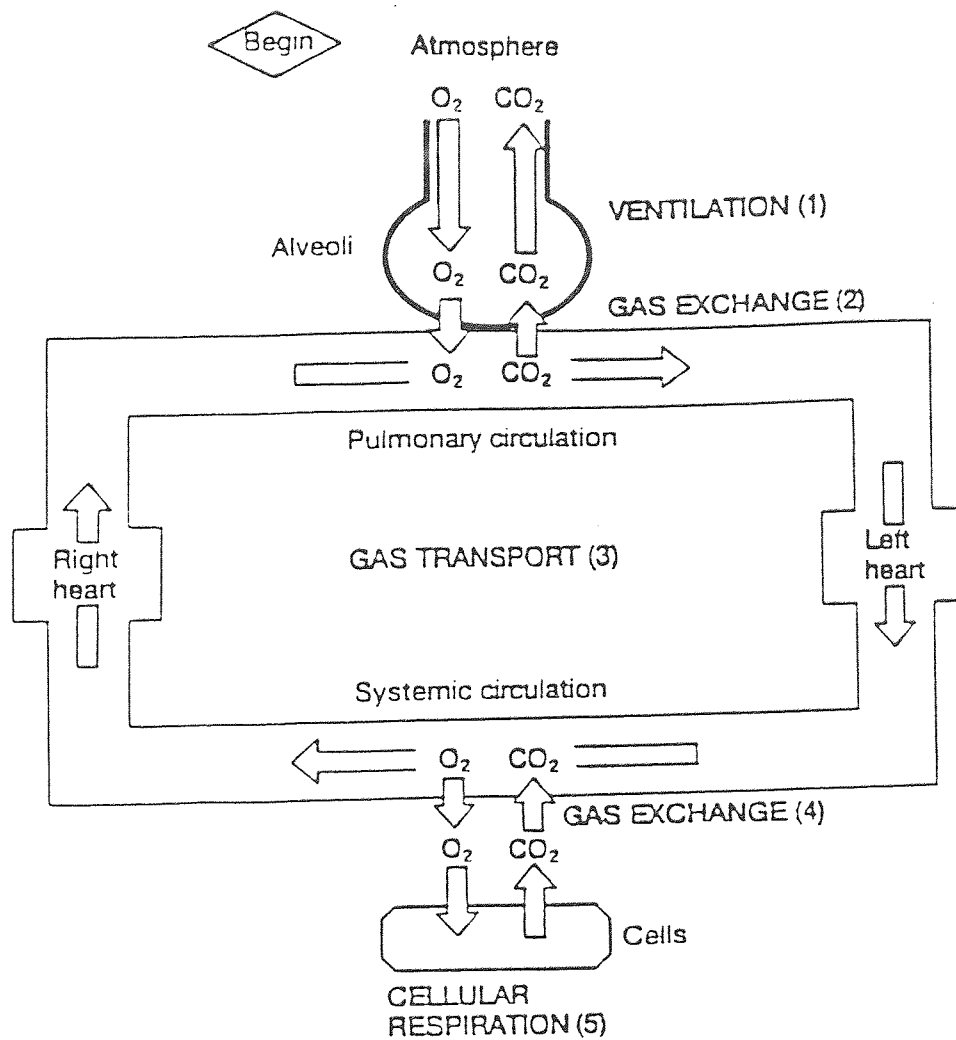


Figure 1.7 Steps of respiration

Just before inspiration begins, the respiratory muscles are relaxed, and no air is flowing since $P_{alv} = P_{atm}$. Inspiration is initiated by the contraction of the diaphragm and the intercostal muscles.

The most important muscle of inspiration is the diaphragm (Figure 1.8) which consists of a thin, dome-shaped sheet of muscle which is inserted into the lower ribs. When it contracts, the abdominal contents are forced downward and forward, and the vertical dimension of the chest cavity is increased. In addition, the rib margins are lifted and moved out by the intercostal muscles, causing an increase in the transverse diameter of the thorax. In normal tidal breathing, the diaphragm moves about 1 cm, but on forced inspiration and expiration, a total excursion of up to 10 cm may occur[55].

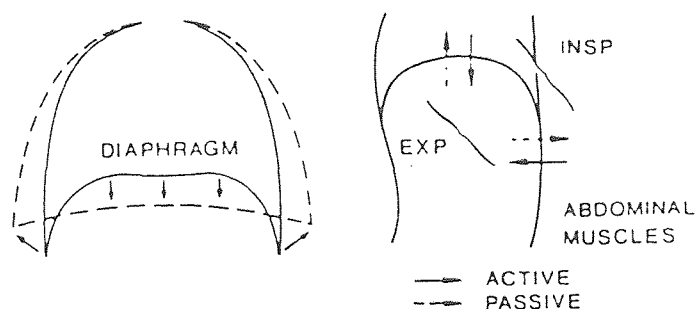


Figure 1.8 Muscles of respiration

The external intercostal muscles (Figure 1.9) connect adjacent ribs and slope downward and forward. When they contract, the ribs are pulled upward and forward, causing an increase in both the lateral and anteroposterior diameters of the thorax. As the thorax enlarges, the thoracic wall moves slightly farther away from the lung surface and the intrapleural fluid pressure becomes subatmospheric[51]. This increases the transpulmonary pressure. The enlargement of the lung causes an increase in the size of the alveoli throughout the lung. By Boyle's law, the pressure within the alveoli changes to less than atmospheric, which produces the difference in pressure that causes a bulk

flow of air from the atmosphere through the airways into the alveoli. By the end of respiration, the pressure in the alveoli is equal to atmospheric pressure.

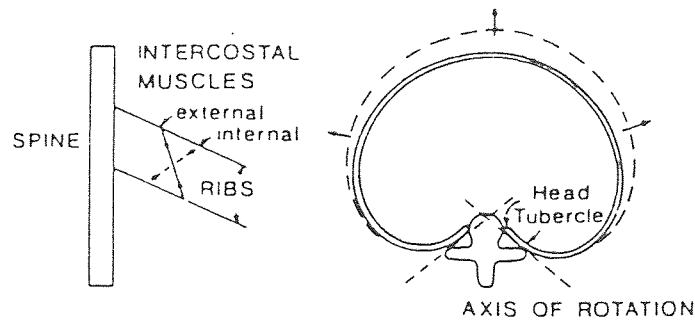


Figure 1.9 Intercostal muscles

Expiration is passive during quiet breathing. The lung and chest wall are elastic and tend to return to their equilibrium positions after being actively expanded during inspiration. During exercise and voluntary hyperventilation, expiration becomes active. The most important muscles of expiration are those of the abdominal wall, including the rectus abdominus, internal and external oblique muscles, and transversus abdominus. When these muscles contract, the intra-abdominal pressure is raised, and the diaphragm is pushed upward. Under certain conditions such as during exercise, expiration of larger volumes is achieved by contraction of the expiratory intercostal and the abdominal muscles, which actively decrease thoracic dimensions.

The pressure-volume curve of an excised lung can be demonstrated with the help of the experiment described below. If an excised lung is placed inside a jar and the pressure inside the jar is reduced to below atmospheric level, the lung expands due to an increase in volume of the chest cage (Figure 1.10a). The graph (Figure 1.10b) shows that the curves which the lung follows during inflation and deflation are different. This behavior is called hysteresis.

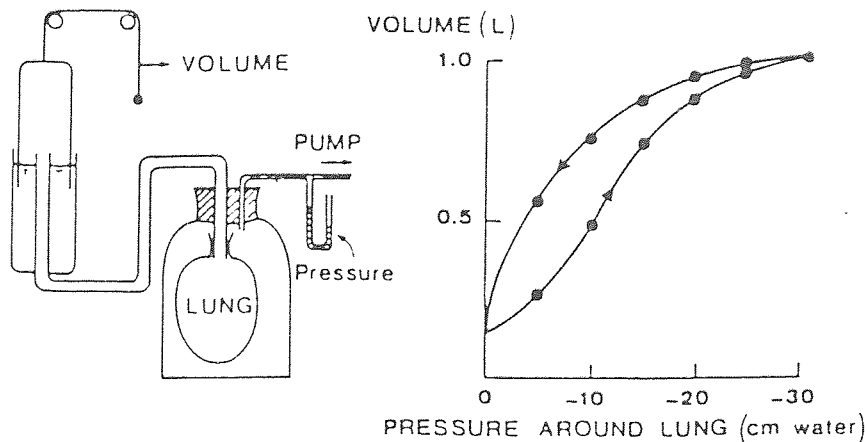


Figure 1.10 Pressure-Volume curve of an excised lung

In the graph of Figure 1.10, the slope of the pressure-volume curve, or the volume change per unit pressure change is called the compliance. Compliance (CL) is defined as the magnitude of the change in lung volume (V_L) produced by a given change in the transpulmonary pressure which is the difference between the alveolar and interpleural pressures[51].

$$CV = \Delta V_L / (P_{alv} - P_{int}) \quad (1.6)$$

Thus, the higher the compliance, the easier it is to expand the lungs at any given transpulmonary pressure.

The surface tension of the liquid film lining the alveoli is another important factor in the pressure-volume behavior of the lung. It is the force in dynes acting across an imaginary line 1 cm long in the liquid surface (Figure 1.11). It arises because the forces between adjacent molecules of the liquid are stronger than those between the liquid and gas, with the result that the liquid surface area becomes as small as possible.

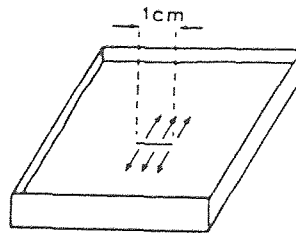


Figure 1.11 Surface tension

Ventilation is defined as the exchange of air between the atmosphere and the alveoli[51]. It has been shown[55] that the lower regions of the lung ventilate better than upper zones. This was demonstrated by having the subject inhale radioactive xenon gas (Figure 1.12). A radiation camera was used to record the radiation penetrating the chest wall. The volume of the inhaled xenon going to various regions was determined. It was seen that the ventilation per unit volume is greater near the bottom of the lung and became progressively smaller toward the top.

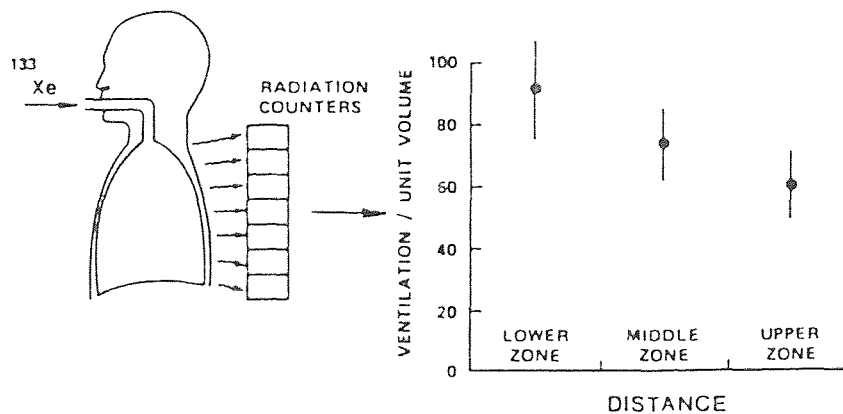


Figure 1.12 Measurement of regional differences using radioactive xenon.

The intrapleural pressure is less negative at the bottom than at the top of the lung due to the weight of the lung. The main cause of regional differences in pressure is the change in volume of air exhaled or inhaled per unit resting volume[55]. The base of the

lung has a larger change in volume and smaller resting volume than the apex. A remarkable change in the distribution of ventilation is found to occur at low lung volumes since the lung at the base is not being expanded but is being compressed, and ventilation is impossible until the local intrapleural pressure falls below atmospheric pressure. By contrast, the apex of the lung is on a favorable part of the pressure-volume curve and hence ventilates well.

The mechanism of uneven ventilation can be explained with the help of Figure 1.13. If the lung is regarded as an elastic chamber connected to the atmosphere by a tube, the amount of ventilation depends on the compliance of the chamber and the resistance of the tube. In the figure, unit A has normal distensibility and airway resistance. Its volume change on inspiration is large and rapid, so that it is complete before expiration for the whole lung begins. Unit B has low compliance and its change in volume is small and rapid. Unit C has a large airway resistance so that inspiration is slow and not complete before the lung has begun to exhale. Inequality of ventilation can result either from alterations in local distensibility or airway resistance, and the pattern of inequality depends on the frequency of breathing.

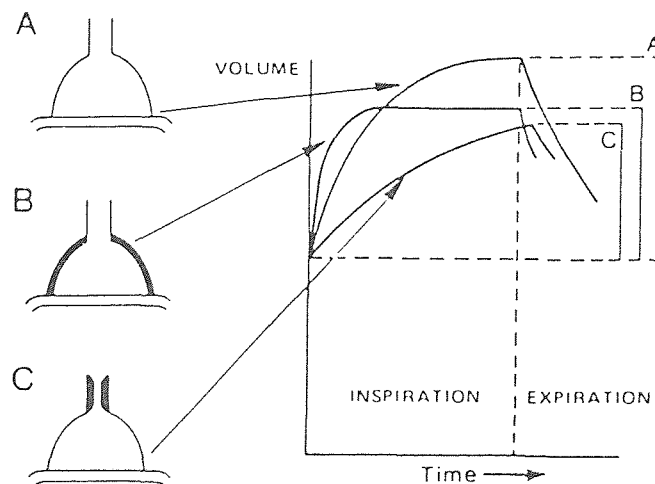


Figure 1.13 Effects of compliance and airway resistance

1.7 Lung Volumes

The lung in a simplified manner can be represented by the Figure 1.14. The various bronchi which make up the conducting airways (Figure 1.6) are represented by a single tube labeled anatomic dead space[51] which leads into the gas exchanging region of the lung which in turn is bounded by the blood-gas interface and the pulmonary capillary blood.

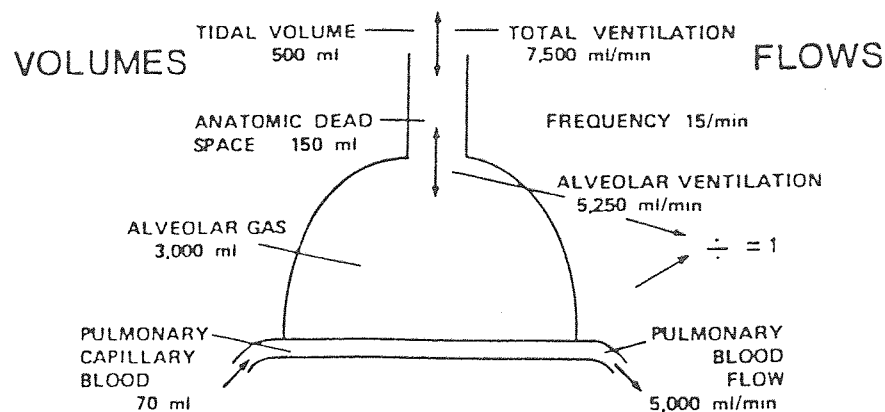


Figure 1.14 Simple representation of the lungs

The volume of air entering the lungs during a single inspiration is, normally, approximately equal to the volume leaving during the subsequent expiration. This is called the tidal volume. During normal quiet breathing, the tidal volume is approximately 500mL[51]. After expiration of a resting tidal volume, the volume of air still contained in the lung is called the functional residual capacity (FRC), which is approximately 2500mL. Through maximal active contraction of the expiratory muscles, it is possible to expire 1500mL of the 2500mL after the resting tidal volume has been expired; this additional volume being the expiratory reserve volume (ERV). After maximal expiration, approximately 1000mL of air still remains in the lungs, called the residual volume (RV). The volume of air that can be inspired over and above the resting tidal volume is called

the inspiratory reserve volume (IRV), which is approximately 3000mL of air. The maximal volume of air that a person can expire, regardless of the time required after a maximum inspiration, is called the vital capacity (VC).

The various lung volumes and capacities recorded on a spirometer, an apparatus for measuring inspired and expired volumes are shown in Figure 1.15. The total lung capacity and RV cannot be measured using the spirometer. The conventional spirometer consists of a bell which moves up and down during expiration and inspiration. The subject is connected to it with a face mask or a mouthpiece into which he breathes. During exhalation, the bell goes up and the pen down, marking a moving chart.

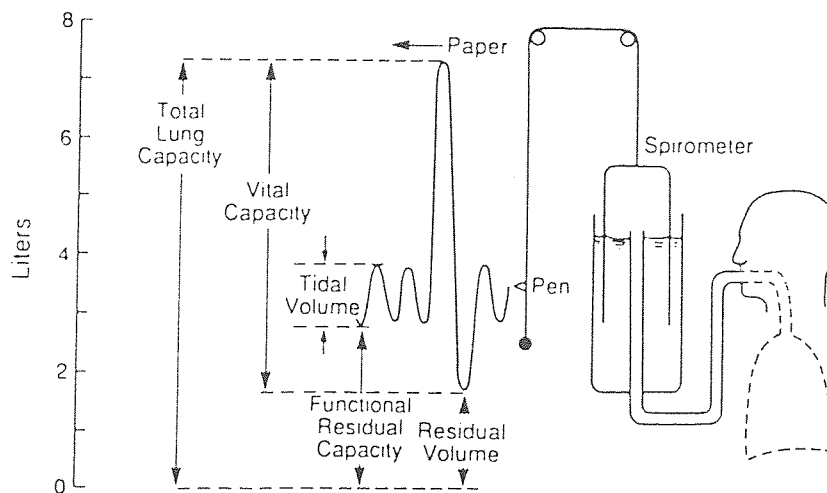


Figure 1.15 Spirometer recording of lung volumes and capacities

1.8 Impedance pneumography

Cremer[12] in 1907, first suggested electrical impedance as a means of studying physiological movements. About 25 years later, Atazler[5], using a modification of Cremer's technique, recognized that breathing caused chest impedance changes. This probably marked the advent of impedance pneumography, a technique which until the seventies failed to gain general acceptance as a useful and valuable tool for research purposes.

The chest impedance pneumograph (IP) works on the principle that with an increase in gas volume of the chest in relation to the extra cellular fluid volume (extra and intravascular), conductivity decreases and the length of the conductance path increases due to expansion, thus increasing the electrical impedance. Theoretically, transthoracic electrical impedance changes (chest movements as the subject breathes in and out), can be used as a noninvasive technique to monitor respiratory changes in lung gas volume (tidal volume), changes in lung water (congestion and edema) and heart rate[20] and cardiac output.

Although there are many methods of detecting respiration, all suffer from disadvantages of the discomfort and inconvenience for the subject, stability, ease of use, simplicity, accuracy, reliability, and sensitivity which limit their application. A technique which is free from many of these advantages is the impedance method which uses the simplest of all transducers, (a transducer is a device which converts one form of energy into another) a pair of electrodes. With these electrodes affixed to the wall of man or an experimental animal, it is possible to detect changes in transthoracic impedance which mirror the respiratory act[6].

Traditionally, respiration is recorded by the use of four instruments, the pneumotachograph, the pneumograph, the spirometer and the negative pressure transducer[23]. Although the pneumotachograph and spirometer are excellent quantitative instruments which indicate air velocity, volume and respiration, both require connection to the air-way by a face mask or mouthpiece. While the true volume is indicated and the resistance to breathing can be made low, a considerable restriction is imposed on the subject. Recording intra-tracheal or intra-pleural pressures with a negative pressure transducer is only practical in a laboratory setting with anaesthetized animals and is relatively difficult to calibrate.

The impedance method for recording respiration offers many practical advantages. The technique (impedance pneumography) is relatively insensitive to

barometric pressure, temperature and force of gravity[23]. One of the major advantages is that the transducer is simple being merely a pair of electrodes. The other important advantage is that because of its location adjacent to the heart, it is possible to obtain the electrocardiogram (EKG) simultaneously, while it is being used to record respiration.

Research has been done by many investigators to decrease some of the difficulties encountered in using the impedance pneumograph[18]. Atazler[5] in 1935, while recording chest-to-back impedance changes reflecting cardiac activity, called attention to respiratory artifacts and avoided recording them by requesting the subject to hold his breath. Fenning[16] in 1936, employed a capacitance technique to record the respiration of a rat and respiratory movements of a rat fetus. In both studies, the animal was placed on one plate of a capacitor, the second plate being placed above, but not in contact with the tissue which moved. Schaefer[48] in 1949, developed an impedance system for recording respiration in man and animals using electrodes inserted subcutaneously in the chest wall. Nyboer[43] in 1959, used impedance plethysmography for recording respiration in rats and called attention to the large respiratory impedance changes evidenced between the torso and limb electrodes. That such impedance changes were related to the volume of air was first established by Goldensohn and Zablow[23] in 1959. who passed a 10KHz current between electrodes on the wrists and detected the respiratory signals from similar electrodes placed further up on each arm.

The block diagram of the equipment used for measuring respiration in this project is shown in Figure 1.16.

A 50KHz oscillator is connected to a large resistor (to provide a constant current source) between the pair of electrodes used as transducers to record both EKG and respiration simultaneously. The output of the oscillator is fed to respiration and EKG filters. The outputs of these in turn are fed through the respiration and EKG amplifiers. The output of the respiration filter is then demodulated and amplified again. The reason

for demodulation of the signal is explained next. The simulated input and output to the system is shown in Figure 1.17 (a and b) respectively.

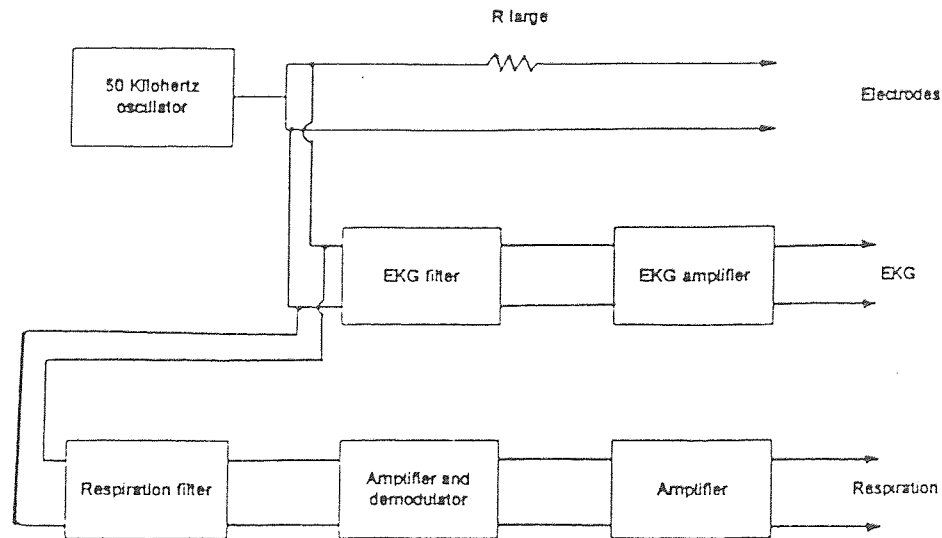


Figure 1.16 Impedance pneumograph

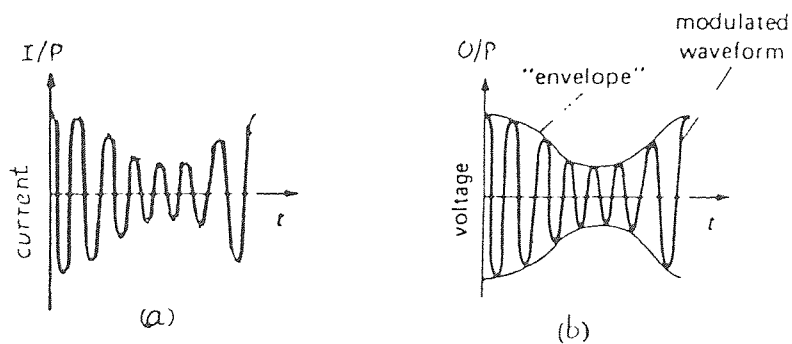


Figure 1.17 Amplitude modulation

The "envelope" in Figure 1.17(b) represents the impedance of the subject. This signal is modulated in amplitude. Since the envelope contains the information that is required, the signal is demodulated before it is amplified again in order to extract the information.

1.9 Prior research

Studies have been performed to quantitatively measure electrical resistive impedance changes of the chest related to pulmonary air volume. Most of the research done in this area was in the early fifties and sixties. The main objective of this project was to replicate previous studies using a different protocol, modern signal processing techniques and better instrumentation.

Even though the concept of measuring impedance changes to study physiological movements was first introduced by Cramer[12] in 1907, most of the important results in this area came into light during the fifties. The movements of the thoracic cage and diaphragm in respiration was explored by Wade[52] in 1953. In the author's project, since respiration is measured by measuring the transthoracic movements, it is important to understand the movement of the thoracic cage. Wade[52] described a method of measuring diaphragmatic movements by screening the movements of the shadow of each dome of the diaphragm on a fluorescent screen as the subject breathed in and out. He conducted this study for the subject in supine and standing positions. He concluded that the relationship between the movement of the diaphragm and the changes of chest circumference and the volume of air ventilated are extremely variable from subject to subject and that the regression coefficients obtained were not statistically significant.

The various physiological and biological factors in impedance pneumography were studied by Powers, Schaffer, Boba and Nahamura[46] in 1958. They used the impedance plethysmograph to measure blood flow quantitatively. They used standard electrical circuits to determine the precise nature and values of electrical properties of biological tissues.

In 1959, Stead, Wells, Gault and Ognanovich[50], conducted research on the conventional spirometer and improved it to obtain greater accuracy. They changed the metal bell used in the conventional spirometer to a light weight plastic bell with chain, and compared the responses of the original and improved spirometers to a simulated fast

breath. They found that the overshoot that occurred at high rates of breathing in the original spirometer improved when the modification was made. These results show that the accuracy of the instruments used plays an important role in different measurements.

Goldensohn and Zablow[23] in 1959 investigated the recording of the changes in torso electrical impedance during respiration in order to obtain a recording of respiration without the physiological and psychological effects. They compared simultaneous impedance and bell spirometer recordings, and were able to obtain relatively accurate recordings of respiratory patterns by impedance spirometry.

Geddes, Hoff, Hichman and Hinds[19] in 1962 were the first of the teams to study the effect of electrode positions on impedance changes when measuring respiration. They found that varying the positions of the electrodes on the chest gave larger or smaller impedance changes for every breath. They also conducted a study to determine the optimum placement of electrodes and found that the posterior electrode position yielded high correlations. Figure 1.18 summarizes the size of the signal recorded on man with electrodes placed at various levels along a midaxillary line. The rib number and the relative breath amplitude are plotted. This study is important to the author's project since the electrodes have to be positioned in a particular position to get optimum results. In the author's project, the results for different electrode positions discussed in Chapter 2 were studied to see which position gave the best result.

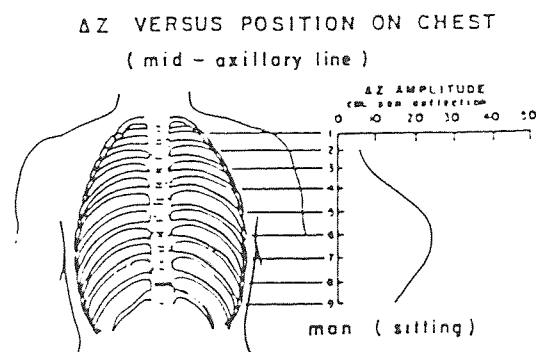


Figure 1.18 Impedance changes versus electrode positions in man

In 1963, studies similar to the author's was done by Allison, Holmes and Nyboer[3]. In these studies, they used electrical impedance plethysmography to measure electrical resistive impedance changes of the chest and compare the results with the volume of air obtained from a respirometer. They conducted experiments on human subjects with electrodes placed in different positions such as wrist-to-wrist, deltoid-deltoid, torso-lumbar region and posterior thorax and found that the posterior thorax position gave the best results. They calculated the resistive impedance changes using the formula

$$R = \rho L / A \quad (1.7)$$

where L = length of the material sample, A = cross sectional area in cm², ρ = resistivity and R = resistance. They concluded that at high inspiratory and forced expiratory volumes, there was less agreement between impedance changes and spirometer volumes. This study gave insight for the author to consider the concept of electrode positioning and its effect.

Logic, Maksud and Hamilton[38] in 1967, discussed the importance of electrode positioning when transthoracic impedance signals were used to measure breathing. They measured the impedance in normal human subjects with electrodes placed at different levels on the midaxillary line. They found that the relationship between impedance change and the inspired volumes was linear only when the electrodes were placed high on the midaxillary line. They also measured chest circumference changes for each electrode position and found that it was linear with inspired volumes only when the strain gages were placed at the fourth or fifth intercostal spaces on the midaxillary line.

Hamilton, Beard, Carmean and Kory[27] in 1967, measured the tidal volume and the total ventilation . A high correlation was demonstrated between transthoracic resistive or capacitive changes and ventilation when special narrow ridged detecting

electrodes were used as transducers. The variability between accumulated impedance changes and ventilation measurements with a spirometer was found to have a standard deviation less than 6% of the ventilation. A linear relationship was demonstrated between lung volume changes and impedance changes for subjects in different positions regardless of the breathing pattern. The author's project deals with similar tests, but using electrodes without narrow ridges.

In 1968, an interesting design was proposed for the conventional impedance pneumograph by Cooley[11]. In the instrument that was being used until then, large impedance changes not directly related to breathing were mixed with the breathing signal. In Cooley's design, a guard ring was used around the measuring electrodes which eliminated the above effect and greatly increased the signal due to breathing. Since lung tissue impedance by itself changes greatly, the small output signals of the conventional pneumograph is caused by substantial fringing currents flowing within the thoracic wall between electrodes and thereby shunting the signal. The guard ring is introduced to supply these currents to insure that the current from the central impedance measuring electrode flows directly through the lung tissue.

Other important studies in this area were conducted by investigators to explain the importance of measuring lung volumes and respiration for clinical purposes. Studies were done by Hirsch and Bishop[29] in 1981, where the volume was controlled and the relation to respiratory sinus arrhythmia (RSA, is defined as the profound influence of heart rate on respiration) was determined. They found that a linear relationship existed permitting normalization of RSA frequency curves for the tidal volume to yield one curve. Mehlsen[41] in 1987, studied the heart rate responses to stepwise and periodic changes in lung volumes in normal controls. He found that the difference between the fastest and the slowest heart rates was significantly larger in response to inspiration than in response to expiration. Detailed studies on impedance plethysmography were done by Powers, Schaffer, Boba and Nahamura[46] in 1958. They used the instrument to measure

resistance for determining blood flow. Weltman and Ukkested[53] in 1969, used impedance pneumography to record signals across the arms and found a strong linear relationship between impedance change and inspired volume for the arm-to-arm measurements. The transthoracic electrical impedance variations associated with respiration in animal subjects was studied by Kira, Yasunobi, Satoshi and Ayao[33] in 1971. The level of ventilation attained and breathing patterns during different types of activities have important clinical implications. Paek and Dennis[44] in 1992 used noninvasive measures of ventilation in subjects performing different activities such as bicycling, lifting, pulling and arm ergometry. They studied cases with and without mouthpieces for the same subject. They concluded that breathing patterns were altered during varied types and intensities of activities. The results of these investigations are important since these will lead to future research and establish the importance of pulmonary measurements using different techniques and use the results for clinical interpretations.

CHAPTER 2

METHODS

2.1 Methods

A physiological signal generated by a biological system (human body) is influenced by physiological parameters such as respiration, blood pressure, and heart rate. In order to understand the processing and analysis of physiological data, the methods of data capture, the instrumentation used, the experimental setup, and the various methods of analysis will be discussed in detail in this chapter.

Two sets of data were involved in the author's study. The first set of data was collected by one of the students working at Kessler Institute for Rehabilitation for her research. The tests for her study involved electrodes placed in a lead II configuration (Figure 2.1). EKG (Electrocardiogram), respiration, blood pressure and volume of respiration were collected for this test. EKG and respiration were collected by impedance pneumography, blood pressure was collected using a Finapres with finger cuffs, and respiration volume was collected using a spirometer. For each subject, seven two minute intervals of data were collected. In the first interval, the subject was requested to rest. Paced breathing at 8, 12 and 18 breaths per minute (bpm) were acquired in the next three intervals. In the remaining intervals, the subject performed paced breathing at predetermined respiration rates while maintaining a specified respiration volume. The paced breathing data were used by the author for her project. Eleven normal subjects, 5 females and 6 males took part in this study. This group was in the age range 20-55 years.

The second set of data was collected by the author, and involved electrode positions other than the lead II configuration (explained below). Six subjects, 3 males and 3 females took part in this study. This group was in the age range 20-30 years. The

subjects were restricted from having caffeine at least an hour before the test. Subjects taking medications were excluded from the study.

The placement of electrodes played a crucial role in this study. Literature review was done on different electrode positions used for similar studies (Chapter 1). Different positions of electrodes were examined to see which particular position gave the optimum correlation (Appendix 2). The subjects were tested in three different postures:

- (1) Sitting
- (2) Standing and
- (3) Supine

The five different electrode positions (Figures 2.1(a), (b), (c), (d), and (e)) used in the test were,

(a) Lead II configuration with one pair of electrodes placed diagonally on the anterior, below the right collar bone and on the rib just below the chest, connected to the impedance pneumograph (Resp 1). A third ground electrode was placed on the left wrist.

(b) Anterior, with one pair of electrodes placed below the left and right collar bones and connected to one impedance pneumograph (Resp1), and the other pair placed on the left and right ribs just below the chest, connected to the other impedance pneumograph (Resp 2).

(c) Anterior, with one pair of electrodes placed below the left collar bone and on the left rib just below the chest connected to Resp1, and the other below the right collar bone and on the right rib just below the chest connected to Resp2.

(d) Posterior, with one pair of electrodes placed on the top portion, connected to Resp1, and the other placed on the bottom portion, connected to Resp 2.

(e) Anterior and posterior positions, with one electrode placed below the right collar bone on the anterior right side and the other, placed on the posterior bottom on the left side.

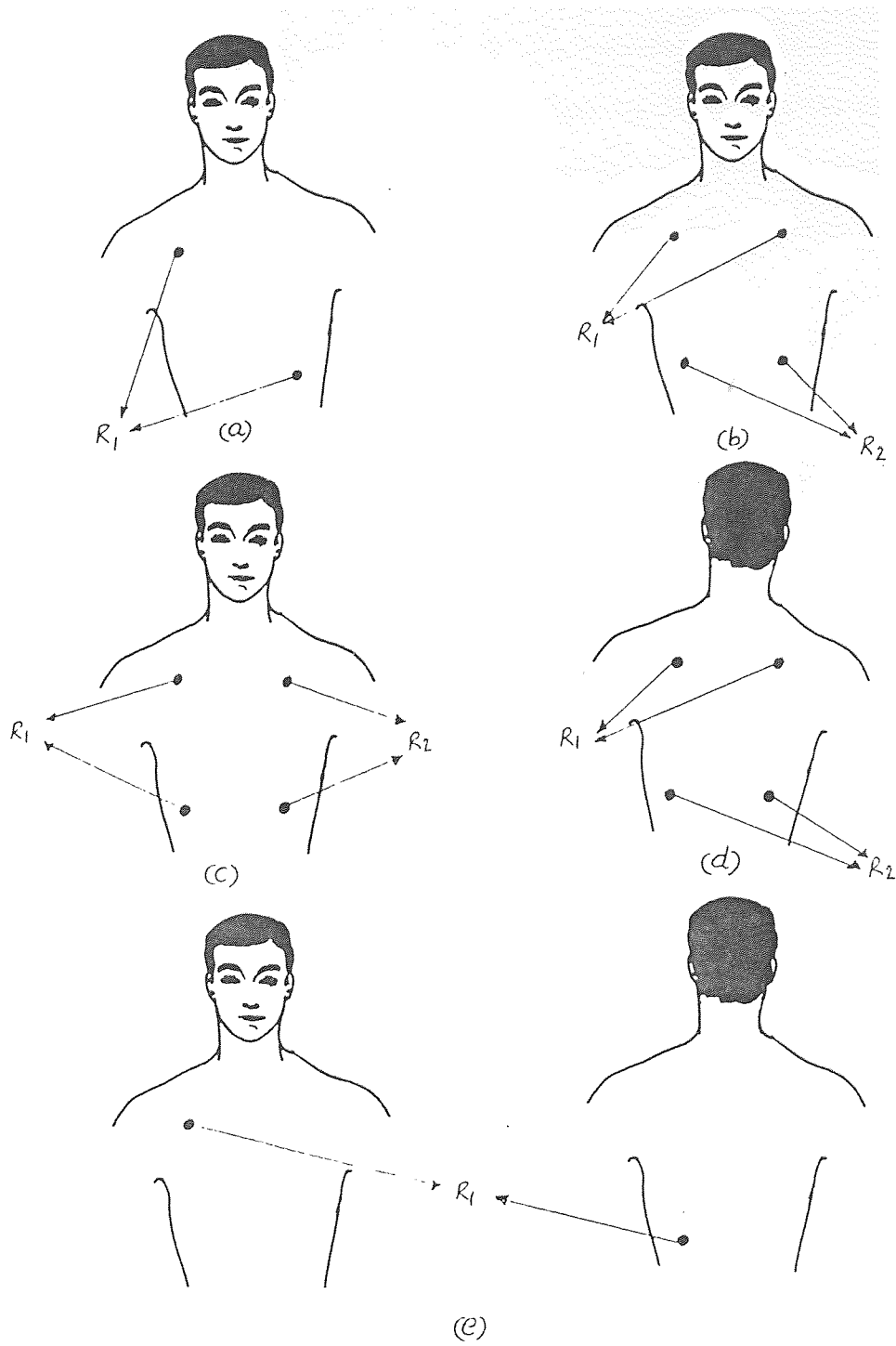


Figure 2.1 Different electrode positions used in the study

The lead II configuration tests were done in the sitting posture only. The other four electrode positions were used to test the six subjects, for all the three postures mentioned above. The skin prep was done by cleaning the skin with alcohol, and drying by abrading gently with a gauze (general-use sponge) to establish good contact with the skin in order to acquire clean signals. The following criteria relating to electrode characteristics were implemented for this study:

(1) The electrodes were placed in a position that minimized movement artifacts related to thoracic respiratory movements.

(2) The electrodes were placed in a manner such that the critical length (30 cm) between them remained a constant.

(3) The electrode position was such that the electrical current distribution covered the pulmonary field.

(4) The signal amplitude was large enough for accurate recording and analysis.

(5) The sensitivity of the impedance pneumograph was fairly constant for a range of ventilatory excursions.

(6) The electrical signal reflected proportional volume changes over the entire range of ventilation.

The experimental protocol used, which is described below, was consistent with the one used for the investigation of heart rate variability studies, which are presently ongoing at the Kessler Institute for Rehabilitation.

Respiration and volume of respiration were collected in subjects during 3 two minute test conditions for all electrode positions mentioned above, other than the lead II configuration:

(1) resting, non-paced breathing

(2) resting, paced breathing at a rate of 8 breaths/minute (bpm), and

(3) resting, paced breathing at a rate of 18 breaths/minute (bpm)

The lead II electrode position involved only pacing files. It included pacing at 12bpm besides pacing at 8 and 18bpm. The subjects breathed through a #7900 two-way mask with low-resistance one-way valve (Hans Rudolph, Kansas city, MO) into a Harvard Dry Gas Meter (spirometer) via low-resistance tubing. A treatment table was used by the subjects for the seated and supine postures. Breathing rate was controlled by visual feedback, by using a view box containing a column of green and red lights that rose and fell at the required breathing rate. The subject was instructed to match his or her breathing rates with the rate at which the lights went up and down the columns. A green light moving up directed the subject to breathe in and a red light moving down directed the subject to breathe out.

2.2 Data Acquisition

Respiration was acquired by an Impedance Pneumography device (Resp I, UFI, Morrow bay, CA). The signal was acquired by impedance pneumography (Chapter 1). The subject was interfaced to the impedance pneumograph with the pair of electrodes acting as the transducers and the resistance between the two electrodes was measured. As the subject breathed in and out, the impedance between the two electrode changed due to the variation in the dimension of the thorax. The first 5000 points of a typical respiration signal obtained using the Resp 1 is shown in Figure 2.2. This signal corresponds to 25 seconds of data (since the sampling rate was 200 per second). The X-axis represents time in seconds and the Y-axis represents the amplitude of the signal in volts.

Volume of respiration was measured with a spirometer. The subject wore a mask which was interfaced to the spirometer. This mask consists of valves that permit the subject to inhale air. The exhaled air passed through a tube connected to the mask, which in turn was connected as the input to the spirometer. The spirometer digitally displayed the total volume of air exhaled. The spirometer recorded tidal volume in the form of pulses and responded only to exhalation. The exhaled volume was recorded in the form

of pulses where each transition corresponded to 0.05 liters of air exhaled. The inhaled volume was represented by the line between the pulses, since the spirometer did not respond to inhalation. The first 5000 points (corresponding to 25 seconds of data) of a typical signal recorded by the spirometer is shown in Figure 2.3. The X-axis represents time in seconds and the Y-axis represented the amplitude of the signal in volts. The pulses represented the volume exhaled and the lines between them represented the volume inhaled at every breath.

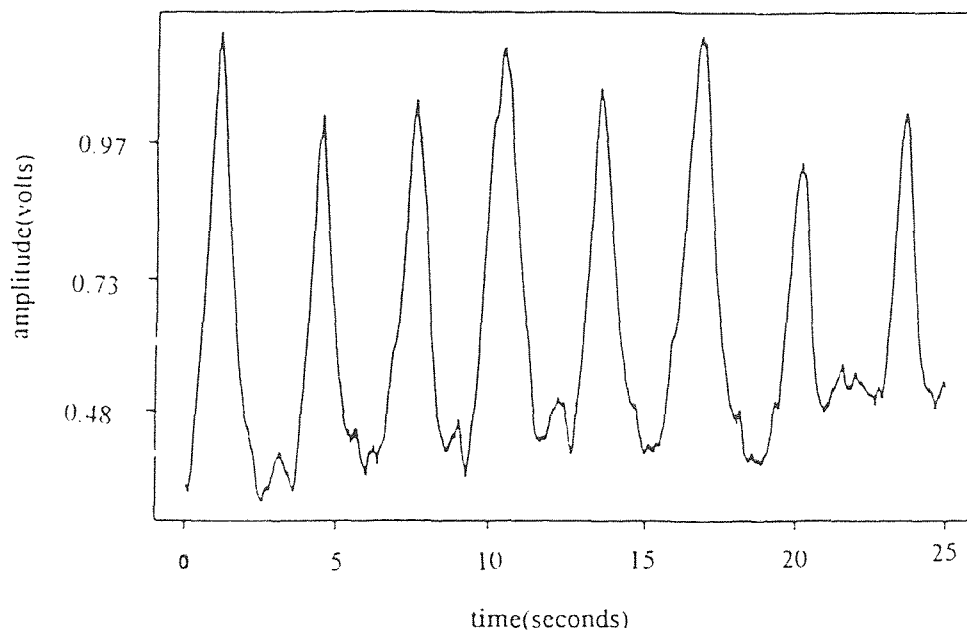


Figure 2.2 Typical respiration signal obtained from the Impedance pneumograph

The output signals were acquired by an IBM compatible 386/40MHz data acquisition computer at a 200Hz sampling rate per channel. The data acquisition computer contained a Keithley Metrabyte DAS-16 analog-to-digital interface board (Appendix 1). The respiration and volume of respiration signals were serially digitized by the data acquisition computer at the same sampling rate and stored sequentially in the form of a binary file which was converted to an ASCII file before being used for analysis.

The PRIMPLOT software was used to preview the signal in real time before acquiring it.

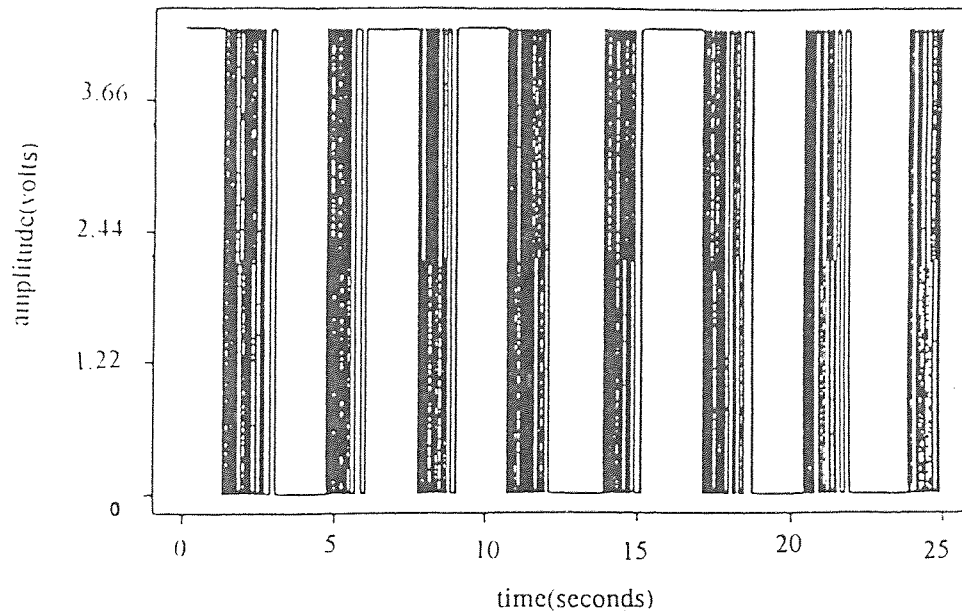


Figure 2.3 Spirometer recording of tidal volume

The impedance pneumograph recorded the respiration signal indirectly by means of impedance plethysmography. A constant amplitude 50KHz current was applied to the chest between the pair of electrodes and the resulting voltages reflecting the impedance changes due to the filling and emptying of the lungs during respiration was detected. The software program used for data acquisition was Streamer version 3.25 by Keithley Metrabyte (Appendix 1).

The data analysis of the signals was performed on an IBM compatible 486/50MHz computer. The software package used for the analysis was S-Plus for windows version 3.1 (Statistical sciences, Seattle, WA). S-Plus is a powerful language which includes modern statistical techniques and permits writing of custom S-Plus programs.

2.3 Signal processing

In order to do the signal processing, the spirometer and the pneumograph signals were superimposed and plotted, for visual observation. Figure 2.4 is an example of the superimposed spirometer and pneumograph signals.

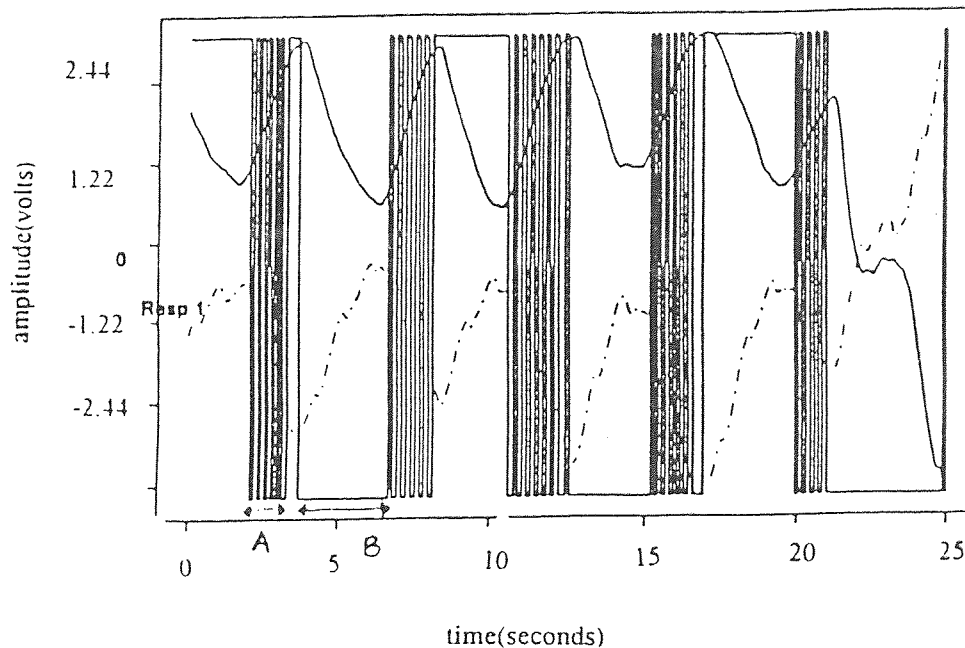


Figure 2.4 Superimposed spirometer and pneumograph signals

In the figure, the signals recorded by the pneumographs, Resp1 (solid lines) and Resp 2 (dotted lines) are superimposed on the signal recorded by the spirometer, for easy visual observation. The signal acquired by Resp 2 (dotted lines) was inverted since the polarity of the electrodes were changed during the test. Traditionally, the spirometer is used to measure tidal volume. The purpose of the author's project was to find an alternative method of measuring tidal volume, that is, to measure it by impedance pneumography (Chapter 1). In order to do that, the signals acquired by the spirometer and the pneumograph were superimposed (Figure 2.4). At each breath, it was seen that the peak

and the valley of the respiration signal occurred in the exhalation (A) or inhalation (B) ranges of the signal recorded by the spirometer. Visual observation of the superimposed signals indicated that the peaks and valleys of the respiration signal consistently occurred in each exhalation (span of a pulse range) or inhalation (span between any two pulse ranges) ranges of the spirometer signal. Therefore, the differences between corresponding peaks and valleys were considered to be equivalent to the volume exhaled. These differences were computed for each case to obtain the tidal volume, and correlated with the tidal volume measured by the spirometer. If good correlation was found to exist, then the spirometer could be eliminated from the study, and the pneumograph can be used to obtain the tidal volume (Chapter 1).

Before the data were analyzed, it was observed that there was some 60Hz noise picked up along with the signal. Therefore, the signal was first smoothed by filtering, using the S-Plus internal function "lowess", at a frequency at which the noise just began to disappear. Figure 2.5 is an example of superimposed spirometer and the filtered pneumograph signals.

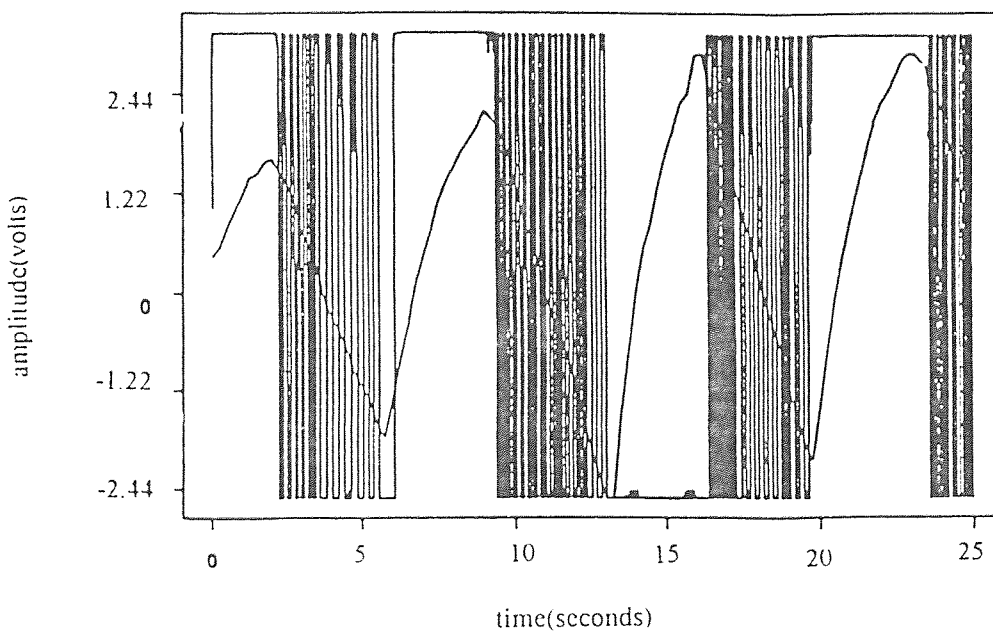


Figure 2.5 Superimposed spirometer and smoothed pneumograph signals

The peaks and valleys of the smoothed signal at each breath were detected, and the corresponding differences were calculated. These differences were then correlated with the tidal volume measured by the spirometer. The correlations (Chapter 3) obtained were very low. Therefore, for future analyses the tidal volume was correlated without filtering the respiration signal. It was observed that the correlations obtained without filtering significantly improved.

2.4 Data analysis

Programs for peak and valley detections, and calculating spirometer tidal volumes were written in S-Plus. Refer to Appendix 3 for the programs. Figure 2.4 is used as an example to explain the analysis using the programs. In order to detect the peaks and the valleys, the exhalation (A) and inhalation (B) ranges of the spirometer signal at each breath were first determined. The maximum (peak) and minimum (valley) values in the computed ranges were obtained. The difference between these values represented tidal volume. The program "POS" was used to determine the exhalation (A) and inhalation (B) ranges of the spirometer signal at each breath. The algorithm is explained in the flowchart shown in Figure 2.6.

The S-Plus programs "PKEX" and "PKIN" were used to detect peaks and the programs "VALEX" and "VALIN" were used to detect valleys that occurred in the exhalation(A) and inhalation(B) ranges of the spirometer signal respectively. The difference between the peaks and the valleys were then calculated to obtain the tidal volume. The algorithm for the programs to detect peaks and valleys is explained in the flowchart shown in Figure 2.7.

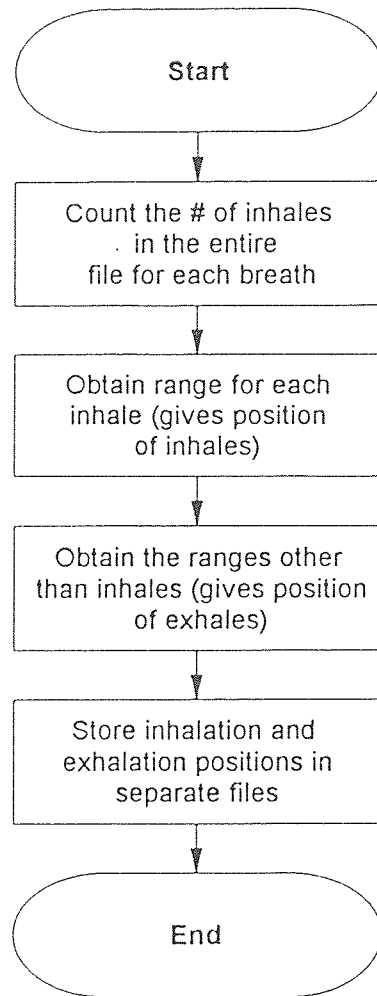


Figure 2.6 Flow chart for obtaining the positions for exhalation and inhalation widths.

"SPIR" was the program used to obtain the tidal volume acquired by the spirometer. Figure 2.4 can be used as an example to explain the program. The spirometer output was in the form of pulse trains that occurred at intervals, where each interval corresponded to an exhalation. The lines between the pulses corresponded to inhalations. The algorithm used is explained with the help of the flowchart shown in Figure 2.8.

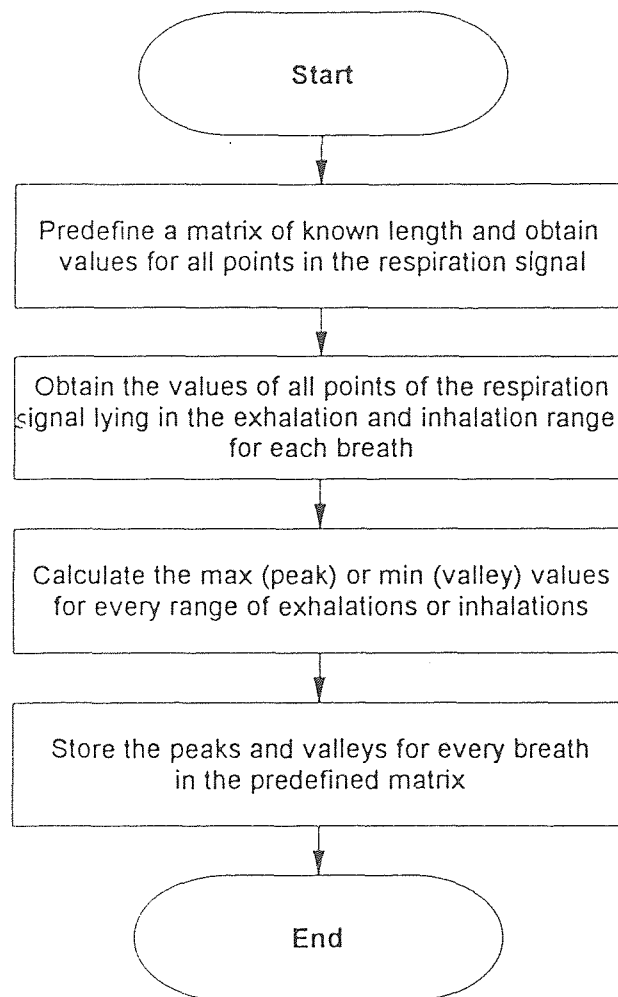


Figure 2.7 Flow chart for obtaining the volume from the pneumograph

"MSD" was the program used to calculate the means and the standard deviations of the pulse widths for each interval. It is explained with the help of the flowchart shown in Figure 2.9.

The program "VOLMAT" is used for obtaining the volume exhaled as calculated by "SPIR" in the form of a matrix in a separate file. The data were analyzed using two different approaches, the first being linear regression, and the second, non-linear

regression(see Chapter 3). Once the difference between the peaks and the valleys (respiratory volume) was obtained, it was stored in a matrix. The exhaled volume at each breath obtained from the spirometer (tidal volume) was also stored in another matrix. The width of the exhalations and the inhalations (differences between the beginning and end values of individual pulse positions) obtained using "POS" was stored in the form of a matrix. The exhalation width, the inhalation width, the mean of the pulse widths, the standard deviations of the pulse widths, and the tidal volumes obtained from the spirometer were then combined into a single matrix with five columns using the internal function "cbind" in S-Plus.

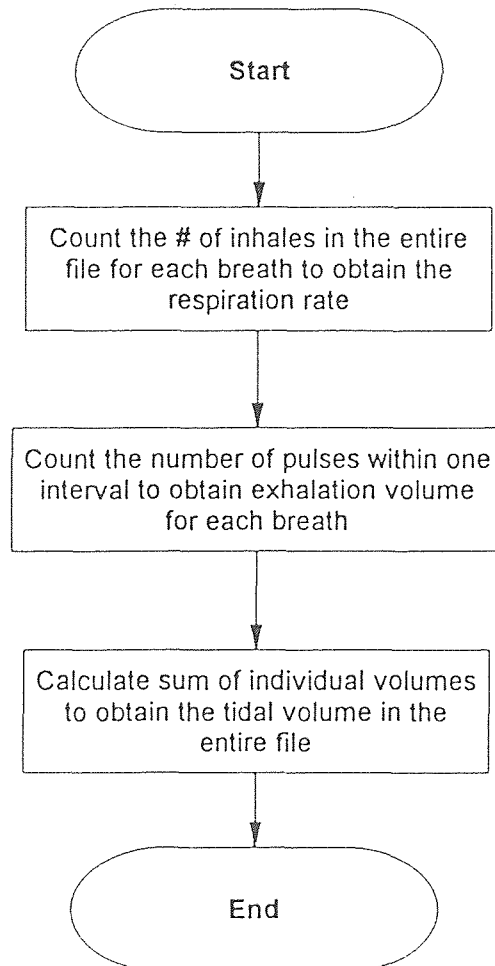


Figure 2.8 Flow chart for obtaining the tidal volume measured using the spirometer.

Care was taken to see that the number of rows in the two matrices to be correlated was the same. The internal functions "cancor" and "gam" in S-Plus were used to obtain the canonical correlations (linear regression) and the residual deviances (nonlinear regression) between the respiratory volume obtained by impedance pneumography and the five parameters discussed above. Refer to Chapter 3 and Appendix 5 for a detailed explanation of the results of correlation and the S-Plus functions used.

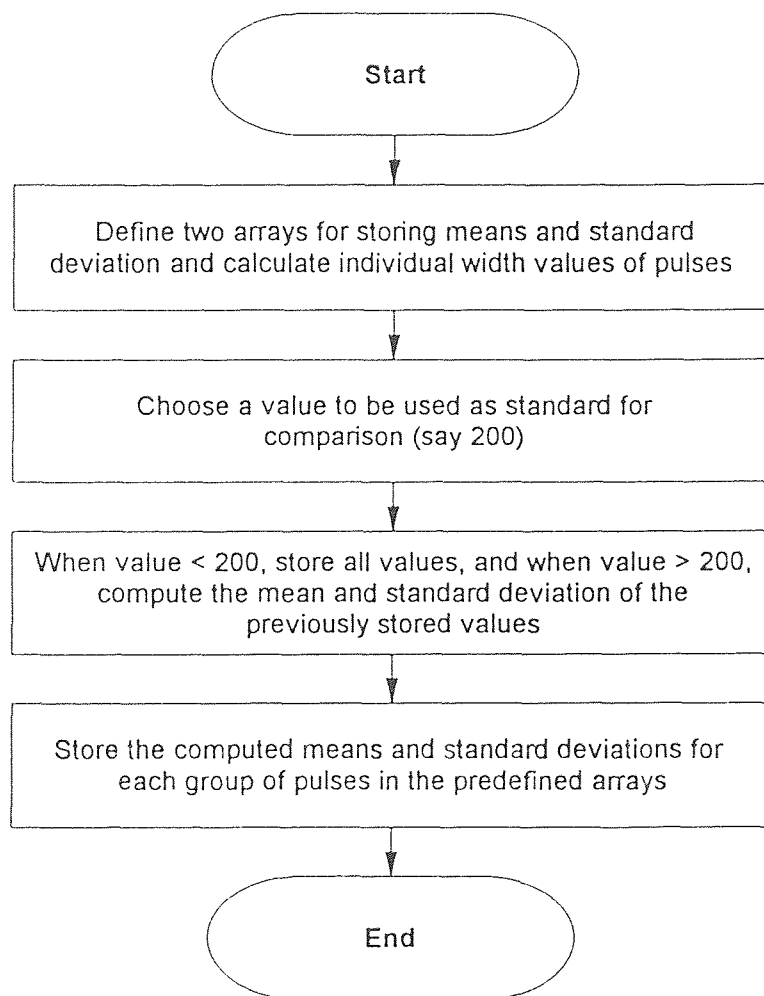


Figure 2.9 Flowchart for obtaining the means and standard deviations of the exhalations

CHAPTER 3

RESULTS

3.1 Frequency response of the impedance pneumograph

One of the possible factors that could affect the correlations between the tidal volume measured by the spirometer and the tidal volume measured by the pneumograph is the performance of the impedance pneumograph (Resp1), which was used as part of the instrumentation for data acquisition. Ideally, the signal input to the Resp 1 should not be changed in shape as it passes through the instrument. In order to verify this, the frequency response of this instrument was tested by performing an experiment in the laboratory. A sudden change in resistance (unit step) using a variable potentiometer was given as an input to the Resp 1, and the frequency response was measured, by measuring the time constant (τ) of the response. A digital oscilloscope was used to record the response of the instrument.

To calculate τ exactly, the following procedure was used. Figure 3.1 shows the response of the instrument.

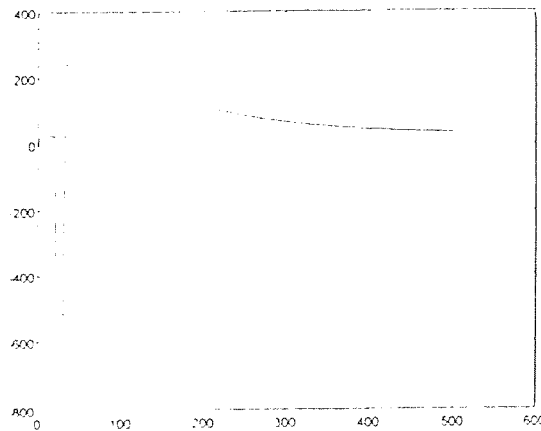


Figure 3.1 Response of Resp1

Assuming that the response was first order, the time constant was calculated, by applying the procedure discussed below. The assumption of first order can be verified by a curve-fitting method called "exponential peeling", which would give an indication of the order of the system. Figure 3.2 shows the typical response of a first order system to a step input. The X-axis represents the time in seconds, and the Y-axis, the amplitude of the signal.

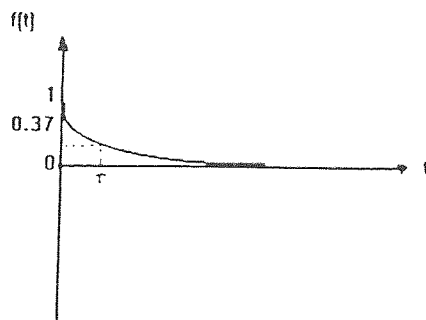


Figure 3.2 First order system response

The equation describing the above system is,

$$f(t) = \exp(-t/\tau) \quad (3.1)$$

where τ = the time constant. At a value of $t = \tau$, the output is

$$f(\tau) = \exp(-1) = 0.37 \quad (3.2)$$

Applying the above principle, the time constant for the actual response of the Resp1 was calculated using Matlab. The time constant was found to be equal to 6.19 seconds, and was used to determine the cut-off frequency (f_c) of a filter which was designed to simulate the response of the Resp1 (Appendix 4). The cut-off frequency was calculated as shown in equation 3.3.

$$\tau = 1/2\pi fc \quad (3.3)$$

The filter was designed using Matlab, and was a fifth order Butterworth high pass filter. Simulated sine waves which represented breathing at different rates starting from 6 bpm up to 20 bpm were simulated and applied as inputs to the filter, and the corresponding outputs were studied. It was found that for relatively low breathing rates (6 and 8 bpm), the output of the filter was attenuated. For rates from 10 to 20 bpm, there was no change in the filter outputs. Figure 3.3 shows the simulated inputs and the corresponding outputs of the filter for breathing at 8, 12 and 18 bpm.

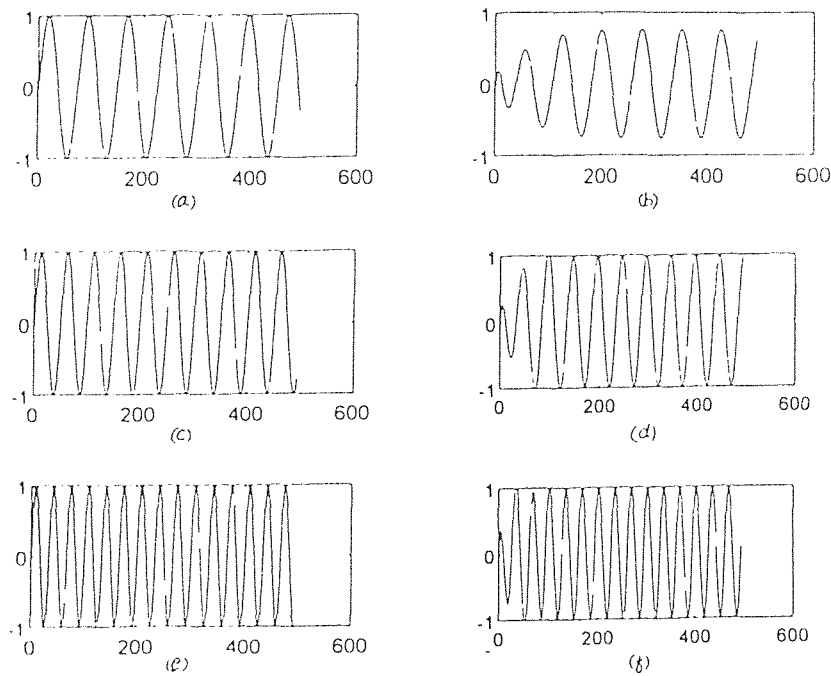
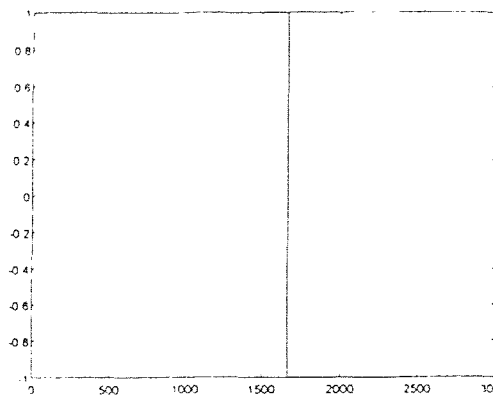
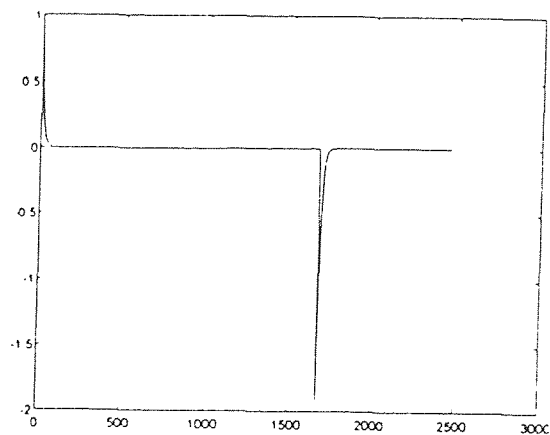


Figure 3.3 Simulated input and the corresponding filter outputs

In order to verify the laboratory experiment for evaluating the performance of the Resp 1, a simulated unit step was constructed using Matlab, input to the above filter (first order), and the resulting response was studied. The time constant was calculated using the method described above, and was found to be 6.17 seconds. Figure 3.4 (a and b) shows the simulated step input and the corresponding filter output respectively.



(a)



(b)

Figure 3.4 Unit step input and corresponding filter output.

The results of breathing at 8, 12 and 18 bpm were important for the author's project, since pacing at 8, 12 and 18 bpm were part of the protocol for the study (Chapter 2). Since only the results of breathing at 8bpm were affected, the percentage attenuation was calculated (Figure 3.3) to be 20 and hence the original signals for pacing at 8bpm were multiplied by 1.25 ($1/(80/100)$) before they were processed. For the resting (non-paced) files which contain many frequencies, the situation becomes very complicated. Theoretically, a different technique explained next should be used to solve the problem. Figure 3.5 shows the inputs, the outputs and the transfer function of a system both in the time and frequency domains.

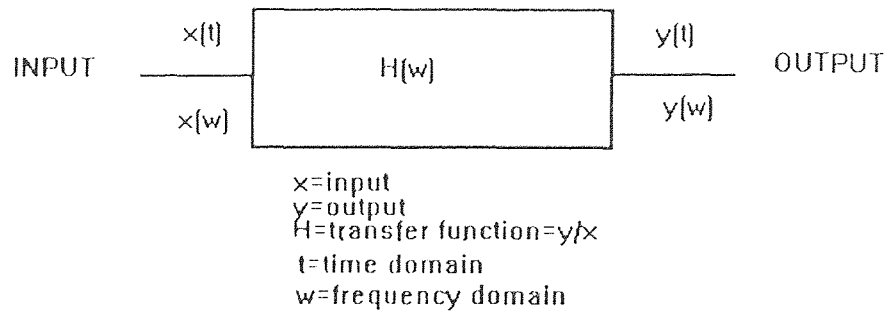


Figure 3.5 Schematic showing the input, output and transfer function of a system in time and frequency domains

The transfer function of this system is given by $Y(w)/X(w)$. Theoretically, if any of the two variables are known, the third one can be determined. In this case, we know $H(w)$, which is obtained from the filter response. We also know the system output $Y(t)$ which is the output of the Resp 1. The output in the frequency domain $Y(w)$ can be obtained by taking the transform of $Y(t)$. Since we now know $H(w)$ and $Y(w)$, $X(w)$ can be obtained from the transfer function formula. The inverse transform of $X(w)$ will give $X(t)$. This theory holds only if the signal is stationary. In this project, since we have

assumed that the signal is stationary, this technique can be applied to solve the problem. This technique is suggested for future work related to this project.

3.2 Lead II electrode configuration results

Eleven subjects, 5 females and 6 males, were tested in this electrode position (Chapter 2), in the sitting posture only. The paced 8, 12 and 18 bpm files of these data were used by the author for her correlation studies. The canonical correlations of the spirometer and the respiratory volumes for these files were calculated using the programs described in Chapter 2, for all 11 cases. Canonical correlation [15] seeks a linear combination of one set of variables versus a linear combination of a second set of variables such that the correlation is maximized. It is a type of linear regression, which seeks a linear combination of a set of variables (tidal volume measured by the spirometer) that maximizes the correlation with a single (response) variable (tidal volume measured by the pneumograph). The data is centered using means. Table 3.1 shows the correlation coefficients for the eleven subjects, when pacing at 8, 12 and 18 bpm.

Table 3.1 Correlation coefficients for the lead II electrode configuration

Subject#	Correlation Coefficient		
	Pace 8	Pace 12	Pace 18
1	0.29006	0.4063	0.08711
2	0.1568	0.2971	0.28526
3	0.4303	0.2526	0.3275
4	0.234	0.2509	0.3251
5	0.1497	0.24098	0.379
6	0.834	0.6789	0.2669
7	0.863	0.8372	0.7534
8	0.5596	0.399	0.37561
9	0.458	0.575	0.4381
10	0.4312	0.4905	0.5379
11	0.331	0.285	0.47881

One of the impedance pneumographs (Resp1) was used for this electrode configuration. No significant conclusions could be drawn from the results, since some of the correlation coefficients (Appendix 2) were high, and some were low. From the results obtained thus far, it was concluded that more electrode positions were to be considered in the protocol with different postures. The protocol was improved by adding more electrode positions and postures (Chapter 2). This led to the second set of results, shown next.

3.3 Linear regression results

The test protocol was changed to resting, pacing at 8bpm and pacing at 18bpm. Pacing at 12 bpm was excluded from the protocol at this stage since, from the results obtained thus far, it was observed that pacing at 12 bpm did not yield important information. Also, it would have increased the duration of the test, which was already lengthy. Three different postures were incorporated:

- (1) Sitting
- (2) Standing
- (3) Supine

Each posture was tested with 4 different electrode positions (Chapter 2) which were:

- (1) Anterior
- (2) Lateral
- (3) Posterior, and
- (4) Anterior and posterior combination.

Six subjects, 3 females and 3 males were involved in this study. Canonical correlations were obtained for the 6 cases, for all electrode positions and postures. To begin with, the respiratory volume (peak and valley differences, Chapter 2) for this study was initially correlated only with the spirometer volume (tidal volume). The results of these correlations were found to be low (not shown). However, other factors besides the

tidal volume which were thought to influence the correlations were now included in the study. It was important to consider as many parameters as possible, in order to improve correlations. Every time a new parameter was added and the correlations computed, the correlations were seen to improve significantly. The tidal volume measured by the spirometer was finally correlated with:

- (1) Spirometer volume for every breath
- (2) The width of each individual exhalation pulse group
- (3) The length of the line between the pulses (Chapter 2), which represented inhalation
- (4) The mean of the widths of all the transitions in a pulse group at each breath, and
- (5) The standard deviation of the widths for individual pulse groups

The Table 3.2 shows the correlation results for one subject when the respiratory volume was correlated with the 5 parameters discussed above. Tables 3.3-3.7 (Appendix 6) show the correlation results for the remaining subjects. The correlations improved significantly (four fold) compared to those obtained when only the spirometer volume was correlated (coefficients of spirometer volumes versus the respiratory volume are not shown). It was concluded that the posterior electrode position gave optimum results for the seated and standing postures and that the lateral electrode position gave optimum results for the supine posture.

Table 3.2 Linear regression results for subject #1

SUB #1			
POSTURE	*PRO+EP	LINEAR	REGRESSION
		(CANONICAL CORRELATION)	
		R1	R2
SITTING	R.1	0.2436	0.3111
	P8.1	0.7286	0.61889
	P18.1	0.5741	0.5893
	R.2	0.3692	0.826
	P8.2	0.7672	0.7183
	P18.2	0.5951	0.6724
	R.3	0.444	0.2691
	P8.3	0.7841	0.7531
	P18.3	0.883	0.7162
	R.4		0.2111
	P8.4		0.7852
	P18.4		0.4165
STANDING	R.1	0.3511	0.4029
	P8.1	0.5382	0.5062
	P18.1	0.4724	0.3812
	R.2	0.7222	0.3216
	P8.2	0.612	0.8102
	P18.2	0.4106	0.3026
	R.3	0.6204	0.72
	P8.3	0.895	0.7474
	P18.3	0.6715	0.4772
	R.4		0.562
	P8.4		0.64
	P18.4		0.5133
SUPINE	R.1	0.7991	0.6868
	P8.1	0.7759	0.6918
	P18.1	0.7519	0.5866
	R.2	0.6926	0.6221
	P8.2	0.7442	0.7618
	P18.2	0.6548	0.7789
*EP=ELECTRODE POSITIONS			R=REST
1=ANTERIOR			P8=PACING AT 8BPM
2=LATERAL			P18=PACING AT 18BPM
3=POSTERIOR			R1=RESP1
4=ANTERIOR AND POSTERIOR			R2=RESP2

3.4 Nonlinear modeling

Nonlinear regression algorithms were used for further analysis of the same data. When many physiological variables are involved, it becomes difficult to understand the behavior of the system. System modeling becomes necessary when the internal structure of any particular system is not clear. Nonlinear modeling of the system was performed to see the behavior of the system.

System modeling is useful in numerous ways[9], such as allowing development of well-defined mathematical equations that simulate the model. Other advantages of system modeling[9] are listed below.

- (1) better comprehension of a system
- (2) simplification of a complicated system since many real and complex systems can be simplified into a mathematical model with the basic characteristics of the system
- (3) quantile analysis of a system using known parameters in a mathematical model
- (4) abstraction or generation of real system behavior under a condition that is theoretically possible, but practically hard to implement.
- (5) utilization of well-developed theories

In order to model a system, we need to know and understand the characteristics of the system. Since the author's project revolves around respiration, the characteristics of the signal must be studied in order to use a model. Respiration is a periodic signal that consists of well balanced, alternating and smooth expiration and inspiration movements. Hence, it is relatively easy to model the system.

The generalized additive model (GAM) was used for the study. The GAM uses an adaptive approach to model the terms nonparametrically using a scatter plot smoother[9]. The output of GAM, being graphical in nature, can be used to suggest nonlinear system behaviors.

The generalized form of the additive model is as follows:

$$n(x) = f_1(x_1) + f_2(x_2) + \dots + f_p(x_p) \quad (3.4)$$

where x_i and f_i ($i=1,2,3\dots p$) are the predictors and the transform functions of the predictors respectively. The $n(x)$ term contains different parameteric functions, which may be polynomials, logarithms, sinusoids, step functions and other functions. These functions generally add together to fit the data or fit the data in a piece wise fashion[9]. The additive model is very flexible in that it allows us to choose different functions to fit the real data. The GAM uses statistical techniques to simulate real data. The quality of the simulation depends on how many predictors are considered in the model and the type of transform used. An increase in the number of predictors improves the accuracy of the model, but makes the model complex. Selection of the transform is done by comparing the deviances of the models using the different transform functions. The smaller the deviance, the better the model[9]. It is very difficult to determine the right transform function for a chosen variable, and combine it in a corrective way to do the modeling. This makes the use of parametric transform functions less popular. The complexity of this method can be reduced by using regression algorithms. The parametric equations in equation 3.3 are replaced by the nonparametric regression fitting functions, which are basically scatter plot smoothers described below in detail. The nonparametric transforms locally fit the data, and hence require lot of processing time. In order to make the technique easier to apply, it should be supported by a well-developed software. In the author's study, S-Plus was used to do generalized additive modeling.

The nonparametric functions used for the author's project were:

A. `gam(formula)`: This function is used to generate the fit of the GAM. The argument "formula" of the GAM function is of the form

$$output \sim f(input_1) + g(input_2) + \dots + h(input_n) \quad (3.5)$$

where f,g,.....,h are the scatter plot smoothers. The inputs 1,2, and n are the given data sets related to the output.

B. poly(x,n): The function "poly" is a smoothing transform function which generates a basis of polynomial regression. The argument "x" of the function is given data or a predictor. The argument "n" is a parameter used to specify the degree of the polynomial transform.

C. s(x,df): The function "s" is a smoothing transform using the spline method. The argument "x" is the same as in B. The argument "df" is used to specify the degree of freedom of the smoothing transform.

D. lo(x,span, degree): This function is a scatter-plot smoothing transform and uses the robust locally linear fit. The argument "x" is the same as in B. The argument "span" specifies the range of a neighborhood of data points to be included. The argument "degree" has two values; degree=1 indicates a local linear fit while degree=2 indicates a local quadratic fit. Refer to Appendix 5 for details of these functions in S-Plus. The output of the GAM gives numbers for degree of freedom, residuals and the residual deviances. The value of the degrees of freedom represents the total number of data points simulated, and the residual value represents the difference between the actual and simulated data. The residual deviance value is the summation of the square of the residuals. The additive models that were used in this project were:

(1) $\text{gam}(\text{resp.vol} \sim \text{lo}(\text{spir.vol}) + \text{lo}(\text{exhalation width}) + \text{lo}(\text{inhalation width}) + \text{lo}(\text{mean of pulses for each individual pulse group}) + \text{lo}(\text{standard deviations of pulses for each individual pulse group}))$

(2) $\text{gam}(\text{resp.vol} \sim \text{s}(\text{spir.vol}) + \text{s}(\text{exhalation width}) + \text{s}(\text{inhalation width}) + \text{s}(\text{mean of pulses for each individual pulse group}) + \text{s}(\text{standard deviations of pulses for each individual pulse group}))$

(3). `gam(resp.vol~poly(spir.vol)+poly(exhalation width)+poly(inhalation width)+poly(mean of pulses for each individual pulse group)+poly(standard deviations of pulses for each individual pulse group)`

The spirometer volume, exhalation widths, inhalation widths, mean and standard deviations are the different predictors of the respiratory volume. "lo" is a robust locally weighted regression, "s" is a spline smoothing algorithm, and "poly" is a transform generating a basis for polynomial regression (Appendix 5 for details). Table 3.8 is an example of the results of GAM for a particular file, which used spirometer volume and the exhalation widths as the predictors.

Table 3.8 Results of the GAM model using three transform functions, and two predictors

TRANSFORMS	DEGREES OF FREEDOM	RESIDUALS	RESIDUAL DEVIANCES
<i>lo</i>	36	24.8	186633.5
<i>s</i>	36	27	196121.3
<i>poly</i>	36	33	226964.9

The quality of the fit is evaluated by the residual deviance values. The table indicates that different transforms have different residual deviances. The model using the "lo" transform is the best since it gives the smallest deviance compared to the other two transforms. Larger number of predictors help in reducing the residual deviances and thereby making the model good, but they also increase the model complexity. Table 3.9 is an example of the results of GAM for the same file, which used all the five predictors discussed above.

Table 3.9 Improved Results of the GAM using different transform functions, and five predictors

TRANSFORMS	DEGREES OF FREEDOM	RESIDUALS	RESIDUAL DEVIANCES
<i>lo</i>	36	13.26	97620.18
<i>s</i>	36	14.99	131135.1
<i>poly</i>	36	30	221143.2

By comparing tables 3.8 and 3.9, we can see that the residual deviance values have been reduced due to an increase in the number of predictors. The individual contributions of the five predictors used in the model are graphically represented in Figure 3.5.

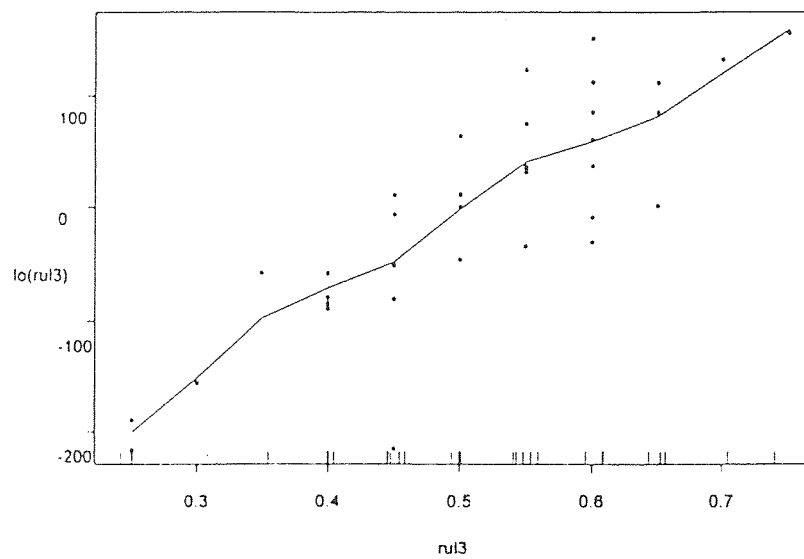


Figure 3.6 (a). Contributions of the five predictors for the example in table 3.9 using "lo" transform; rul3=spirometer volume

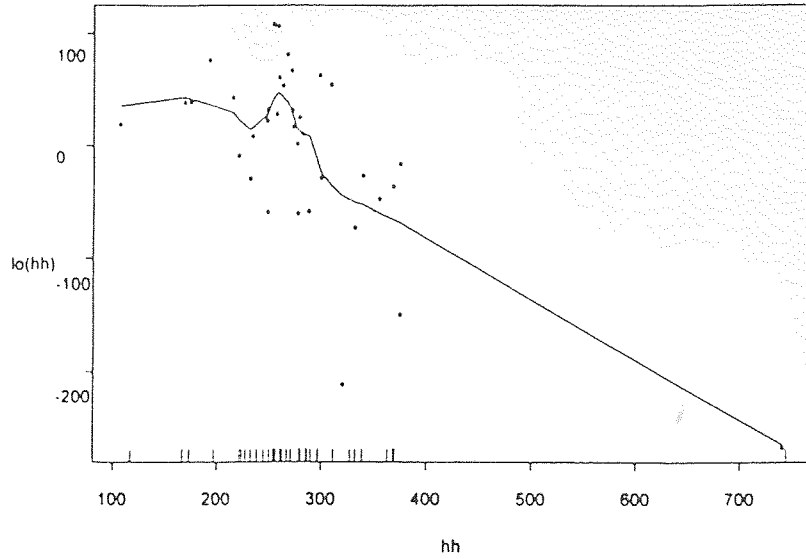


Figure 3.6 (b). Contributions of the five predictors for the example in table 3.9 using "lo" transform; hh=exhalation width

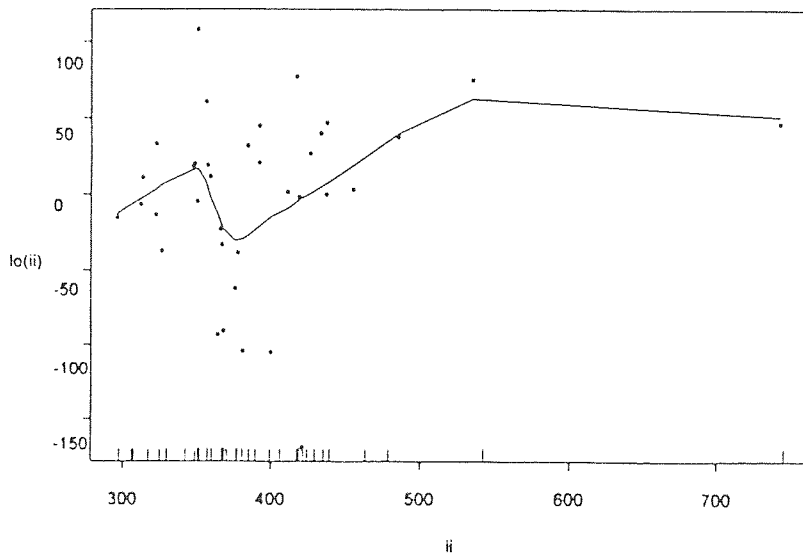


Figure 3.6 (c). Contributions of the five predictors for the example in table 3.9 using "lo" transform; ii=inhalation width

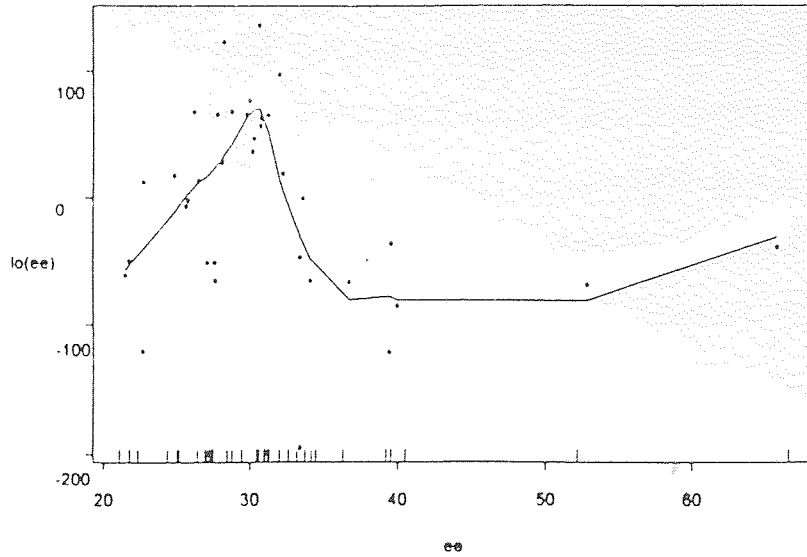


Figure 3.6 (d). Contributions of the five predictors for the example in table 3.9 using "lo" transform; ee=mean of individual widths

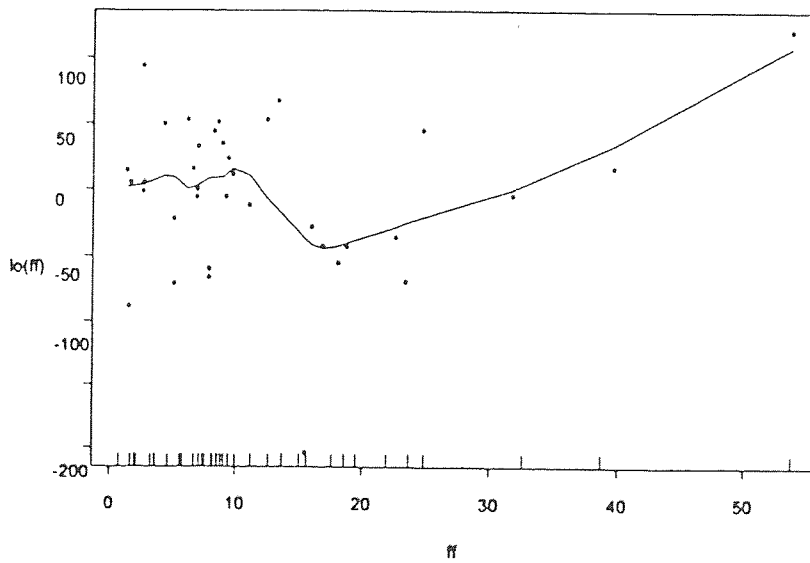


Figure 3.6 (e). Contributions of the five predictors for the example in table 3.9 using "lo" transform; ff=standard deviations of individual widths.

In the figures, the solid lines represent the contribution of the five predictors to the respiratory volume. In Figure 3.6(a), an increase in the value of the spirometer volume produces an increase in the respiratory volume. The relationship is approximately linear as shown by the solid line. In Figure 3.6 (b), the contribution of the inhalation width is cyclical in that the respiratory volume increases and decreases, and then remains a constant with increase in the exhalation width scale. In Figure 3.6(c), the decrease in exhalation width produces a decrease in the respiratory volume. In Figure 3.6(d), the contribution of the means is similar to that in (b). In Figure 3.6(e), the standard deviation produces a decrease and then an increase in respiratory volume with increase in the standard deviation scale. It can be concluded that for the above example, the spirometer volume and the exhalation width play a major role in the respiratory volume correlation. Future work is necessary to physiologically interpret the interesting trends observed in the remaining parameters (inhalation widths and the means and standard deviations of the exhalation widths). The GAM is a useful tool which suggests nonlinearities of the predictors in the system, which can be graphically represented. Table 3.10- indicates the results of the GAM using the three different transform functions applied to one of the 6 subjects. Tables 3.11-3.16 (Appendix 6) indicate the GAM results for the remaining subjects.

It was concluded from these results that the "lo" transform function is the best, since it gave the smallest deviance values. The results were similar to those obtained using linear regression algorithms. It was concluded that the posterior electrode position relatively gave the optimum fit or the best correlations for sitting and standing postures, while the lateral electrode position gave optimum results for the supine position, for all six cases.

Table 3.10 Nonlinear regression results for subject#1

SUB #1							
POSTURE	*PRO+EP			NONLINEAR	REGRESSION		
				RESIDUAL	DEVIANCE	(GAM)	
		R1(LO)	R1(S)	R1(POLY)	R2(LO)	R2(S)	R2(POLY)
SITTING	R.1	123.55	1564	45898.23	12314	58489.23	665489
	P8.1	395.44	1141.34	39124.18	14875.98	52465.47	342743.3
	P18.1	165879.23	120045.3	124478	48970.16	54348.09	1168990.8
	R.2	4582.12	1897.58	48965.58	45689	41235.21	112568.56
	P8.2	288.32	1716.6	47528.33	149.12	823.8	28186.39
	P18.2	45298.13	47322.24	92946.41	39183.71	41075.82	68274.2
	R.3	102.33	115.12	1245	235.12	456.23	12569
	P8.3	22971.56	37669.67	430657.6	33958.88	48176.46	204021.5
	P18.3	17153.68	22963.88	38879.21	3270.21	6979.728	19295.83
	R.4				45698	77548.85	125698.66
	P8.4				7675.597	17238.35	65811.08
	P18.4				150087.8	155841.6	251828.1
STANDING	R.1	1254.55	55898.23	236987	55898	88974.58	125489.25
	P8.1	380.87	3288.21	29393.77	2932.88	18693.36	139481.5
	P18.1	29897.83	38398.57	88014.24	406238.1	453949.5	1016715
	R.2	4234.11	5896.88	456231.25	8976.55	98765.4	201458.58
	P8.2	2252.4	8122	48232.19	15641.54	28955.22	445098.3
	P18.2	62935.96	72707.03	117015	50501.11	63483.25	117814.1
	R.3	5899.23	6425.223	17584.22	4588.02	28798	297855.02
	P8.3	10280.05	62058.93	142343	23858.21	198975.9	394248.9
	P18.3	104816.7	113121.2	291848	49358.75	52715.13	167778
	R.4				48759	87459.25	117889.02
	P8.4				824.46	11322.96	134954.8
	P18.4				43293.95	50549.13	107045.2
SUPINE	R.1	4505.11	9878.33	156486.3	5504.21	9887.03	125325.22
	P8.1	2444	8880.08	147518.5	4501.52	22052.08	103065.1
	P18.1	59630.14	68441.83	149809.1	33248.57	41060.08	92486063
	R.2	356.22	4589.99	154623	224.22	5608.32	156423.8
	P8.2	1908.14	5653.2	58115.55	29357089	135129.2	685740.8
	P18.2	17587.34	23986.55	48458.98	59123.13	74145.48	156470.9
*EP=ELECTRODE POSITIONS		R=REST					
1=ANTERIOR		P8=PACING AT 8BPM					
2=LATERAL		P18=PACING AT 18BPM					
3=POSTERIOR		R1=RESP1					
4=ANTERIOR AND POSTERIOR		R2=RESP2					

CHAPTER 4

DISCUSSION AND CONCLUSIONS

4.1 Discussion

The major finding of our correlation studies was that the posterior electrode position yielded optimum correlations (linear regression) and residual deviances (nonlinear regression) for the seated and standing postures, while the lateral electrode position gave optimum correlations and residual deviances for the supine posture.

The project was a part of the ongoing research in heart rate variability (HRV) at Kessler Institute for Rehabilitation. The HRV study at Kessler deals with the exploration of the relatively elusive autonomic nervous system in a noninvasive manner. The technique used is carried out using power spectral analysis. The objective of the HRV studies is to diagnose and predict neurocardiac disorders. The research protocol for the above study involves the acquisition of various physiological parameters such as respiration, volume of respiration, blood pressure, and EKG. For the HRV project, the EKG is acquired by the impedance pneumography technique where a pair of electrodes is used as transducers, respiration volume is acquired by the spirometer, blood pressure is acquired using a Finapres and finger cuffs. The goal of the author's project, which is a part of the HRV project, was to obtain the volume of respiration using an alternative technique, that is, impedance pneumography. The tidal volumes were obtained using two different techniques, spirometer measurements and impedance pneumography. Statistical analysis methods (linear and nonlinear regression) were used to quantitatively evaluate the data and correlation studies were performed. The objective of the author's study was to eliminate the spirometer from the HRV protocol, since, if good correlations were found to exist, eliminating the spirometer would in turn eliminate the use of a face mask

which was used to interface the subject to the spirometer . This would make the testing procedures easy and the subject comfortable.

Seventeen normal human subjects (males and females) were tested for this study. The experiments were performed in three stages. The protocol for the first stage involved paced breathing at 8, 12 and 18 bpm in the seated posture (lead II electrode configuration). These data were collected by one of the students working at Kessler (Chapter 2). The data were used by the author to compute correlations of the tidal volume measured by the spirometer and the respiration volume measured by impedance pneumography using the procedure discussed in Chapter 2. The results at this stage indicated that no significant conclusions could be arrived at, since there were some high and some low randomly distributed correlation coefficients.

The second set of results were obtained by conducting experiments on six normal subjects, three males and three females, using the rest, pacing at 8 and 18 bpm protocol for sitting, standing and supine postures. The results obtained at this point were examined using a linear regression algorithm by calculating canonical correlation coefficients. The results of linear regression showed improved correlation coefficients compared to that of the lead II electrode configuration. The results of linear regression indicated that the posterior electrode position yielded relatively good correlations in the seated and standing postures, while the lateral electrode position yielded good correlations for the supine posture. There are many factors which must be considered in this study which may play major roles in improving the correlations, which are discussed in section 4.3 of this chapter.

The nonlinear regression approach was used in the third stage for the same data (second stage), since a nonlinear regression algorithm was thought to provide a better fit because many physiological parameters were involved. The GAM (Chapter 3) was used to determine the system behavior. Results of the GAM were similar to those of linear

regression. By using the GAM, the individual contributions of different parameters and their behaviors correlated with the tidal volume were extracted.

In this project, the correlation results obtained for the lead II configuration showed that in general, the correlations were low. For these data, the tidal volume measured by the spirometer was correlated with the tidal volume measured by the pneumograph. To begin with, the respiration signal acquired by the pneumograph was filtered to eliminate the 60 Hz noise and then correlated with the spirometer tidal volume. The correlations were very low (not shown). Then correlations between the spirometer tidal volume and the unfiltered respiration signal were computed. The results were found to improve for all the cases (table 3.1). Therefore, all correlations were computed using the unfiltered respiration signal.

At this time, other possible factors which would influence the correlations such as the exhalation and inhalation widths of the spirometer (Figure 2.3), the mean and standard deviations of the exhalation widths of the spirometer output (Figure 2.3) were computed. Whenever a new parameter was added, the correlations improved significantly. Linear regression algorithms were used to obtain canonical correlations of the tidal volume measured by the pneumograph and the additional parameters discussed above. There was a four fold increase in correlations due to the additional parameters. For the second stage, data were collected by the author for the electrode positions was found that the posterior electrode position gave best correlations for the seated and standing postures while the lateral position gave the best correlations for the supine posture.

An interesting idea was to approach the analysis using nonlinear modeling to investigate if results would be improved. The GAM (Chapter 3) was used for this purpose. The protocol was the same as that used for linear regression. The data were analyzed using the "gam" function. This technique outputs residual deviances which indicate the fit of the data. The advantages of using the GAM was that it could suggest

nonlinearities in the system parameters, which could graphically be represented. This provides better understanding of the system parameter behavior. The results obtained using the GAM (tables 3.10-3.15) were similar to those of linear regression, that is, the posterior electrode position is the best for the seated and standing postures and the lateral position, for the supine posture.

The correlations obtained could further be improved if factors not considered in this study are included. These additional factors are discussed in section 4.3. Studies related to the thoracic cage movements similar to those done by Wade[52] can be conducted to better understand the physiology of the respiratory system. The fact that the diaphragm movement and its relationship to the volume of air ventilated are extremely variable from subject to subject may also influence the results. Wade[52] had concluded in his studies that there was no statistically significant relationship between the chest movement and the volume of air ventilated. Our results showed that the posterior electrode position was relatively the best. But if the other factors (discussed in section 4.3) influencing the system are taken into account, there are good chances of improvement of results.

The impedance pneumography technique could be applied to measure blood flow quantitatively, after studying the physiological and electrical properties of biological tissues. It has many applications in clinical studies. The accuracy of the spirometer is another area that was not studied during the course of this project. If some tests to measure the accuracy of the spirometer can be conducted, then based on the results, there is a chance of improving the correlations. The position of electrodes on the chest is critical since impedance measurements are greatly influenced by the underlying amounts of fat and muscle tissue. The contact between the electrodes and the chest wall is another issue, since if there is no good contact, fluctuations obtained in the readings may influence correlation results. Moreover, the movement of the subject also has an effect in the impedance readings. Cooley[11] used a guard ring around the measuring electrodes

to eliminate these fluctuations in the impedance readings. Hamilton et al.[27] looked at the relationship between transthoracic capacitive changes and ventilation. This could be another area where impedance pneumography can be applied. A comparison could then be done to see the variations in results when capacitance is measured as opposed to resistance. The protocol could be changed so that it includes exercising, performing different activities like bicycling, lifting, pulling and arm ergometry. Cooley[11] has also shown that the impedance measurements are affected by the position of the electrodes over the lung, that is, impedance measurements differed when made at the apex of the lung from those obtained from the base of the lung. Hence, a multiple electrode system should be considered in attempt to record signals simultaneously.

Theoretically, impedance changes represent different volumes of lung tissue in different subjects. Studies done by some investigators have pointed out that in large individuals with thick thoracic walls, current paths have relatively larger diameters and, therefore, larger volumes of lung tissues are penetrated than in lean individuals. The thick chest wall decreases specificity in measuring the electrical properties of the lung both in localization and in conductivity. This is based on the effect of chest wall thickness upon electric current flow. Our experimental set includes positioning the electrodes at certain regions on the subject. But since each person is anatomically different, this aspect would play an important role in affecting the correlations.

Studies have shown that electrode types, structures and characteristics considerably affect the data collected. Several types of electrodes have been used by different investigators like the guard ring design proposed by Cooley[11], and the narrow ridged electrodes used by Hamilton et al.[27].

There are also different aspects related to the author's project which were not examined such as controlling the volume, deep respiration, and exercising. Wade[52] described a method of measuring diaphragm movement and showed that with changes of posture, the extent of diaphragmatic movement in both quiet and deep respiration varied

little, but the resting level of the diaphragm at the end of a quiet respiration changed greatly and the pattern of diaphragmatic movement in relationship to this resting level showed great changes.

Many researchers have attempted to use electrical impedance pneumography as a new monitor for respiration (Allison et al.[3], Baker and Geddes[6], Cooley[11], Goldensohn and Zablow[23], Hamilton et al.[27], Logic et al.[38], and Weltman[53]). They showed unanimously that the impedance increases on inspiration and decreases on expiration which is demonstrated in Figure 4.1 [33].

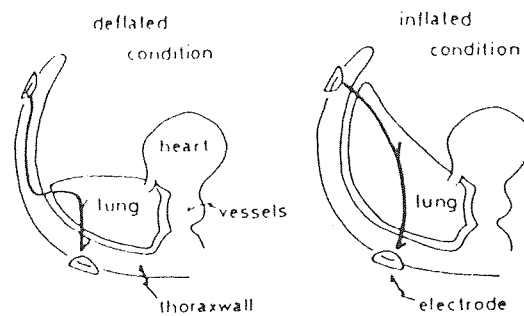


Figure 4.1 A schematic representation of probable pathway of the current across thorax wall during deflated and inflated conditions in a dog.

Further, it has also been observed that impedance variations during respiration recorded from specially selected electrode positions on the thorax are quite similar in pattern with the spirometer and quantitatively related to the variations in the spirometer. In spite of these experimental results, the source of electrical impedance changes associated with the lung volume variations is not definitely clear[33]. Studies conducted by many researchers [11,23,27,38,53] attributed the impedance variations to changes of the lung resistivity associated with lung tissue aeration. Allison et al.[3] considered it to be a manifestation of blood volume within the lung and resulting variations in tissue resistivity associated with respiration. Baker and Geddes[6] concluded that the thoracic

geometry modifications during ventilatory movements are more effective in causing impedance changes than the aeration of the lung. These are some of the areas which were not studied by the author and which if studied, would provide valuable insight.

Even though the results of the author's project indicate that the posterior electrode position gave optimum correlations, if all the other issues mentioned above were to be studied, the results may be significantly improved. Besides the work done thus far, these additional factors should be considered for the complete understanding of the system behavior.

Subsequent investigations will have to determine the precise dependence of the author's technique on different postures and positions, different breathing modes, and different test protocols. Different methods adopted by different researchers can be studied to answer the same basic question "Are the tidal volumes measured by different techniques well correlated?". This would give an opportunity to validate and verify our results.

4.2 Conclusion

Correlation between the tidal volumes measured by the spirometer and the chest impedance changes measured by impedance pneumography at any given time and for any given person are quite good. The results from the author's study indicated that the correlations are relatively good for the posterior electrode position for the seated and standing postures, and the lateral electrode position for the supine posture. However, because of many factors that would influence these correlations, and that were not studied, it is concluded that the above factors should be considered to obtain improved values for correlations. Once the technique is improved and all pertaining details are studied, impedance pneumography can be used as an effective tool to measure and monitor ventilatory parameters other than tidal volume, and could be used in many important respiration-related clinical applications.

4.3 Suggestions for future research

Measurement of respiration and its related parameters is highly desirable in a large number of clinical and hospital applications. Many investigators have tried different techniques of pulmonary measurements in the past two decades, but there are still some underlying mechanisms which are unknown or are unclear.

There were many variables such as the electrode positions, skin prep, and the subject's physique in the experimental set-up that could have caused deviations in the analysis. Looking at the correlations, many questions arise as to why they are low or high for any particular subject. In this study, some of these questions have been answered, but many more need to be answered in order to fully understand the techniques involved and to obtain valuable insight. The small sample size could limit any conclusion regarding the correlations. Further investigation will be required.

Increase of reliability of the experimental data is another area for further exploration. The data in this study were two minute segments for the three cases, resting, pacing at 8bpm, and pacing at 18bpm. The longer the test duration, the more reliable the data. Hence, if possible, the duration of the test must be increased and different respiratory rates should be studied.

Future studies may profitably be oriented towards the following:

(1) Electrode positions on the chest wall and the details of electrode structure, if applicable since studies have been conducted by investigators where the electrode positions on the chest were varied, which gave larger or smaller impedance changes for each breath.

(2) The spirometer required connection to the airway by a face mask which when used for a lengthy test, makes the subjects uncomfortable. As an outcome of this study, if the spirometer is eliminated, it would reduce the discomfort level of the subject.

(3) One of the major aspects which was considered for this study is a method of combining data obtained from the different electrode positions, and then computing the

correlations. Some preliminary studies were done by the author in this regard, but there was no significant change noticed in the correlations. In future, the data have to be combined in an appropriate way to improve correlations.

(4) The problem of choosing one particular electrode position for all the subjects is difficult, since each person is anatomically different.

(5) In the future, the computer programs could be made more efficient by choosing an optimum algorithm for the desired application.

(6) Studies can be done to investigate using a multiple electrode system to acquire data for the different electrode positions simultaneously. This could improve correlations.

(7) To collect and analyze more data, the number of subjects should be increased, and the conclusions of the present study verified.

(8) Since the electrodes used for detection of bioelectric events are applied to a subject, there is always the risk of pick-up of voltage of power line frequency, especially if the subject is in an area in which there is exposed wiring or power devices drawing high currents. Care should be taken to minimize these effects.

(9) Tests should be done to determine the reproducibility of results in a single person.

(10) Artifacts caused by gross movements by the subject during the test should be minimized

(11) The signal processing software can be optimized to improve operations and shorten the processing time involved.

(12) In the future, abnormal subjects should be included in the study since the objective of this is to apply this method to study abnormal subjects. Subjects who are not normal, particularly having pulmonary diseases, would be a group to study. Basically, the diseases of the lung can be classified into one of the following:[55]

A. Obstructive diseases

B. Restrictive diseases

C. Vascular diseases

D. Infectious diseases

A. *Obstructive diseases* of the lung are extremely common. All these diseases are characterized by airway obstruction. The most common types are:

(1) *Airway obstruction*

The lumen is partly blocked, the airway wall is thickened, or the abnormality is outside the airway. Figure 4.2 shows the mechanisms of obstruction due to the reasons explained above.

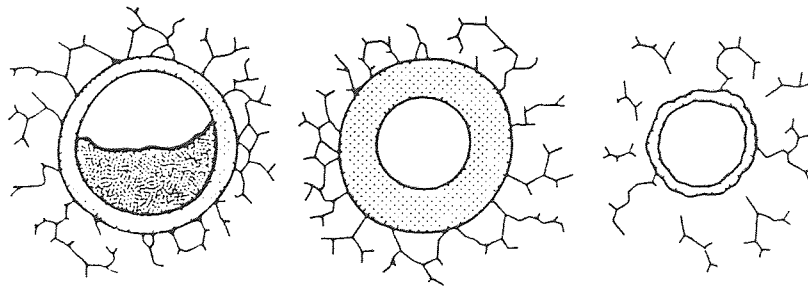


Figure 4.2 Mechanisms of airway obstruction

(2) *Chronic obstructive lung disease*

This includes two main diseases- *emphysema* characterized by enlargement of the air spaces distal to the terminal bronchiole with destruction of their walls, and *chronic bronchitis*, characterized by excessive mucus products in the bronchial tree, sufficient to cause excessive expectoration of the sputum[15].

(3) *Asthma*

This is characterized by increased responsiveness of the airways to various stimuli and manifested by widespread narrowing of the airways. Figure 4.3 shows a

diagrammatic sketch of the different bronchial walls for a normal person and an asthmatic.

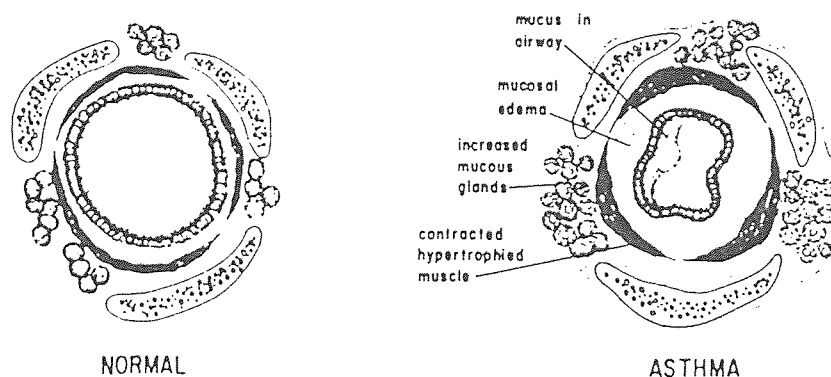


Figure 4.3 Bronchial wall in a normal and an asthmatic

(4) *Localized airway obstructions* which can be classified into *tracheal* and *bronchial*, both caused by an inhaled foreign body.

B. *Restrictive diseases*

These are diseases in which the expansion of the lung is restricted either because of alterations in the lung parenchyma or because of the dysfunction of the pleura, the chest wall, or the neuromuscular apparatus. They are characterized by small resting lung volumes. The types of restrictive diseases are:

(1) *Diffusional interstitial pulmonary fibrosis*

The principle feature of this disease is thickening of the interstitium of the alveolar wall. the airway resistance at a given lung volume is normal or decreased because the retractive forces exerted on the airway walls by the surrounding parenchyma are abnormally high (Figure 4.4).

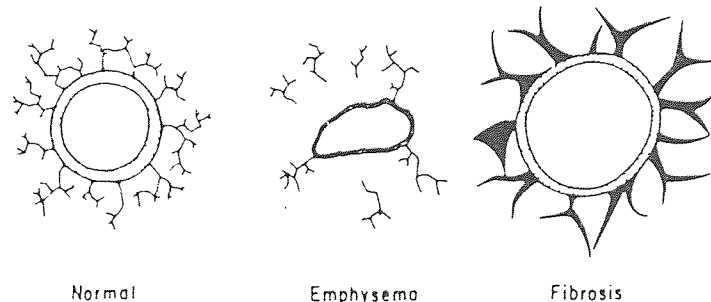


Figure 4.4 Forces exerted on airway walls by the surrounding parenchyma in normal condition, emphysema, and fibrosis.

(2) *Sarcoidosis*

This is characterized by the presence of granulomatous tissue having a characteristic histological appearance and often occurring in several organs.

(3) Diseases of the pleura such as *Pleural effusion* and *thickening*.

(4) Diseases of the chest wall such as *Scoliosis*, *Kyphosis*, and *Ankylosing Spondylitis*, which are characterized by the bony deformity of the chest. *Scoliosis* and *Kyphosis* refer to the lateral and posterior curvatures of the spine respectively. In *Ankylosing Spondylitis*, there is a gradual but relentless onset of immobility of the vertebral joints and fixation of the ribs and as a result, the chest wall movement is greatly reduced.

(5) *Neuromuscular diseases* which affect the muscles of respiration or their nerve supply, which include *Poliomyelitis*, *Guillan-Barre syndrome*, *Amyotrophic lateral sclerosis*, *Myasthenia gravis*, and *muscular dystrophies*. All these can lead to *dyspnea* and respiratory failure.

C. *Vascular diseases*

They are characterized by increase in fluid volumes.

(1) *Pulmonary edema*, which is characterized by an abnormal accumulation of fluid in the extra vascular spaces and tissues of the lung.

(2) *Pulmonary embolism*, which is due to the stasis of blood, alterations in the blood coagulation system, and abnormalities in the vessel wall.

(3) *Pulmonary hypertension*, which is characterized by an increase in the mean pulmonary-artery pressures (normal pressure=15mmHg).

(4) *Pulmonary arteriovenous fistula*, which is characterized by an abnormal communication between the pulmonary artery and a vein.

D. *Infectious diseases like Pneumonia and Tuberculosis.*

Subjects with such diseases should be included in the future study, since the results of such studies can be used as an important tool for clinical interpretations.

APPENDIX 1

Data Acquisition

Prior to acquiring data, files had to be created for storing the data . The signal outputs were interfaced to the computer for subsequent analysis. These signals were connected through an interface box to a Keithley-Metrabyte DAS-16 board, which is a 16 channel analog-to-digital converter. The analog signal outputs were interfaced through different channels of the DAS-16. For actual data acquisition, a data acquisition software called Keithley-Metrabyte Streamer was used. Data was collected and stored using Streamer. The MKFILE command was used to create the storage files in advance. Their sizes were calculated using the formula

$$FS(\text{bytes}) = (SR/\text{channel} * NC * TS * 2) \quad (\text{A.1})$$

where FS = file size

SR = Sampling rate

NC = number of channels

TS = total sampling time (secs)

The sampling rate used for each channel was 200 Hertz. Files for each event in the protocol were two minutes long. The data collected was in binary form. Before using the data for analysis, it was converted into ASCII format using the UNPACK command, and scanned in a matrix form into S-Plus. Each column in the matrix contained the sampled and digitized data from the corresponding channels on the DAS-16.

APPENDIX 2

Correlation

It is important to define covariance in order to know the meaning of correlation. Covariance is a measure of how two random variables vary together either in a sample or in the population, when the values of the two random variables occur in pairs[15].

When the covariance is divided by the product of the estimated sample populations, the result is the correlation, a dimensionless number that measures the strength of the linear association between the two variables.

$$r = \text{Covariance} / \text{product of estimated sample populations} \quad (\text{B.1})$$

where r = correlation coefficient. If all the points lie on a straight line with positive slope, the correlation is 1; if they all lie on a line with negative slope, the correlation is -1. A non-zero relationship between two variables does not necessarily imply a causal relation between them. A correlation of zero implies no straight line association, but there may nevertheless be a curvilinear association.

APPENDIX 3
S-Plus programs

PKEX

```
function(x, y)
{
  k <- 1
  n <- length(x)
  m <- matrix(1:n/2, nrow = n/2, ncol = 1)
  for(j in 1:n) {
    if(k <= n) {
      tp <- seq(x[k], x[k + 1], 1)
      ap <- y[tp]
      bp <- max(ap)
      m[j] <- bp
      print(bp)
      k <- k + 2
    }
  }
  li <- list(m = m)
  li
}
```

PKIN

```
function(x, y)
{
  k <- 2
  n <- length(x)
  m <- matrix(1:n/2, nrow = n/2, ncol = 1)
  for(j in 1:n) {
    if(k < n) {
      tv <- seq(x[k], x[k + 1], 1)
      av <- y[tv]
      bv <- max(av)
      m[j] <- bv
      k <- k + 2
    }
  }
  lis <- list(m = m)
  lis
}
```

VALEX

```
function(x, y)
{
  k <- 2
  n <- length(x)
  m <- matrix(1:n/2, nrow = n/2, ncol = 1)
  for(j in 1:n) {
    if(k < n) {
      tv <- seq(x[k], x[k + 1], 1)
      av <- y[tv]
      bv <- min(av)
      m[j] <- bv
      k <- k + 2
    }
  }
  lis <- list(m = m)
  lis
}
```

VALIN

```
function(x, y)
{
  k <- 1
  n <- length(x)
  m <- matrix(1:n/2, nrow = n/2, ncol = 1)
  for(j in 1:n) {
    if(k <= n) {
      tpv <- seq(x[k], x[k + 1], 1)
      apv <- y[tpv]
      bpv <- min(apv)
      m[j] <- bpv
      k <- k + 2
    }
  }
  li <- list(m = m)
  li
}
```

SPIR

```

function(x)
{
  x[x > 1000] <- 2000
  x[x < 1000] <- 0
  rlength <- rle(x)$length
  rval <- rle(x)$value
  print(paste(rlength, rval))
  #counts packets
  n <- length(rlength)
  packet <- 0
  for(k in 1:n) {
    if(rlength[k] > 200) {
      packet <- packet + 1
    }
  }
  print(paste("the number of inhales is", packet))
  #counts pulses
  rlength[rlength < 200] <- 0
  rlength[rlength > 200] <- 1
  rpulse <- rle(rlength)$length
  print(paste(rpulse))
  vol <- ((rpulse + 1) * 0.05)
  vol[vol == (0.1)] <- 0
  print(paste(vol))
  t <- length(vol)
  count <- 0
  for(k in 1:t) {
    if(vol[k] > 0) {
      count <- count + 1
    }
  }
  print(paste("The count is", count))
  svol <- sum(vol)
  print(paste("the sum is", svol))
  mvol <- svol/count
  print(paste("the mean is", mvol))
  inf <- list(vol = vol)
  inf
}

```

POS

```
function(x)
{
  x[x > 1000] <- 1500
  x[x < 1000] <- 0
  rlength <- rle(x)$length
  print(rlength)
  sum <- cumsum(rlength)
  print(sum)
  aa <- diff(sum) > 200
  bb <- grep(T, aa)
  cc <- sum[bb]
  dd <- sum[bb + 1]
  ee <- append(cc, dd)
  ff <- sort(ee)
  print(bb)
  print(cc)
  print(dd)
  print(ee)
  print(ff)
  rval <- rle(x)$value
  print(rval)
  n <- length(rlength)
  print(n)
  packet <- 0
  for(k in 1:n) {
    if(rlength[k] > 200) {
      packet <- packet + 1
    }
  }
  print(paste("inhales is", packet))
  kk <- list(rlength = rlength, rval = rval, cc = cc,
            dd = dd, n = n, packet = packet, ee = ee, ff
            = ff)
  kk
}
```

VOLMAT1

```
function(x)
{
  k <- 1
  n <- length(x)
  m <- matrix(1:n/2, nrow = n/2, ncol = 1)
  for(j in 1:n) {
    if(k < n) {
      s <- (x[k])
      m[j] <- s
      k <- k + 2
    }
  }
  lis <- list(m = m)
  lis
}
```

VOI.MAT2

```
function(x)
{
  k <- 2
  n <- length(x)
  m <- matrix(1:n/2, nrow = n/2, ncol = 1)
  for(j in 1:n) {
    if(k < n) {
      s <- (x[k])
      m[j] <- s
      k <- k + 2
    }
  }
  lis <- list(m = m)
  lis
}
```


MSD

```
function(x)
{
  marr <- 0
  sarr <- 0
  q <- 1
  j <- 1
  val <- 0
  n <- length(x)
  for(k in 1:n) {
    if(x[k] < 200 && x[k] > 0) {
      val[j] <- x[k]
      j <- j + 1
      print(val)
    }
    else if(x[k] > 200) {
      if(j > 1) {
        m <- mean(val)
        print(m)
        s <- sqrt(var(val))
        print(s)
        marr[q] <- m
        sarr[q] <- s
        q <- q + 1
        val <- 0
        j <- 1
      }
    }
  }
  lis <- list(marr = marr, sarr = sarr)
  lis
}
```

APPENDIX 4

Matlab filter design

The steps involved in the design of the filter using matlab 3.0 are:

```
t = [0:0.1:50]; %an index for the X-axis is chosen
```

```
y = sin(2*pi*f*t); %f=frequency, simulates a sine wave with frequency f
```

```
plot(y); %plot input to the filter
```

```
[b,a] = butter(5, fc, 'high'); % fifth order butterworth high pass filter with cut-off  
frequency fc
```

```
r = filter(b,a,y); % output of the filter, a and b are the filter coefficients
```

```
plot(r); %plot filter output.
```

APPENDIX 5

Splus Functions

A. gam function: Fit a Generalized Additive Model

DESCRIPTION:

Returns an object of class "gam" which is a generalized additive fit of the model.

USAGE:

```
gam(formula,family=gaussian,data=<<see below>>,weights=<<see  
below>>,subset=<<see below>>, na.action=na.fail, start=<<see below>>,  
control=gam.control(...), trace=F, model=F, x=F, y=T, contrasts=NULL, ...)
```

REQUIRED ARGUMENTS:

formula: a formula expression as for other regression models. Nonparametric smoothing terms are indicated by s for smoothing splines or lo for loess smooth terms. Additional smoothers can be added by creating the appropriate interface. Interactions with nonparametric smooth terms are not fully supported, but will not produce errors; they will simply produce the usual parametric interaction.

OPTIONAL ARGUMENTS:

family: a family object - a list of functions and expressions for defining the link

trace: logical flag: if TRUE, then the status during each iteration of the fitting is reported.

x: logical flag: if TRUE, then the x matrix is returned as component x.

y: logical flag: if TRUE, then the response is returned as component y.

contrasts: list of contrasts to be used for some or all of the factors appearing as variables in the model formula. The names of the list should be the names of the corresponding variables, and the elements should either be contrast-type matrices (matrices with as many rows as levels of the factor and with columns linearly independent of each other and of a column of one's), or else they should be functions that compute such contrast matrices.

...: all the optional arguments to `lm` can be given including `weights`, `subset` and `na.action`.

VALUE:

an object of class `gam` is returned, which inherits from both `glm` and `lm`. See `gam.object` for details.

DETAILS:

Components can be extracted using extractor functions `predict`, `fitted`, `residuals`, `deviance`, `formula`, and `family`. The output can be modified using `update`. It has all the components of a `glm` object, with a few more. The response variable must conform with the definition of family, for example factor or binary data if `family=binomial` is declared. The model is fit using the local scoring algorithm,

which iteratively fits weighted additive models by backfitting. The backfitting algorithm is a Gauss-Seidel method for fitting additive models, by iteratively smoothing partial residuals. The algorithm separates the parametric from the nonparametric part of the fit, and fits the parametric part using weighted linear least squares within the backfitting algorithm. Although nonparametric smooth terms lo and s can be mixed in a formula, it is more efficient computationally to use a single smoothing method for all the smooth terms in an additive model. In this case the entire local scoring algorithm is performed in Fortran.

REFERENCES:

Hastie, T. and Tibshirani, R. (1990). Generalized Additive Models. Chapman and Hall, London.

EXAMPLES:

```
gam(Kyphosis~s(Age,4)+Number,family=binomial)
```

```
gam(ozone^(1/3)-lo(radiation)+lo(wind.temperature),data =air)
```

```
gam(Kyphosis~poly(Age,2)+s(Start),data=kyphosis.subset=      Number>10)
```

B. glm function: Fit a Generalized Linear Model

DESCRIPTION: Produces an object of class "glm" which is a generalized linear fit of the data.

USAGE:

```
glm(formula,family=gaussian,data=<<see below>>,weights=<<see
below>>,subset=<<see below>>,na.action=na.fail,start=<<see
below>>,control,trace=F,model=F,x=F,y=T,contrasts=NULL,qr=F, ...)
```

REQUIRED ARGUMENTS:

formula: a formula expression as for other regression models, of the form response ~ predictors. See the documentation of `lm` and `formula` for details.

OPTIONAL ARGUMENTS:

family: a family object - a list of functions and expressions for defining the link and variance functions, initialization and iterative weights. Families supported are gaussian, binomial, poisson, Gamma, inverse. gaussian and quasi. Functions like binomial produce a family object, but can be given without the parentheses. Family functions can take arguments, as in `binomial(link=probit)`.

data: an optional data frame in which to interpret the variables occurring in the formula.

weights: the optional weights for the fitting criterion.

subset: expression saying which subset of the rows of the data should be used in the fit. This can be a logical vector (which is replicated to have length equal to the number of observations), or a numeric vector indicating which observation numbers are to be included, or a character vector of the row names to be included. All observations are included by default.

na.action: a function to filter missing data. This is applied to the `model.frame`

...: control arguments may be given directly, see the control argument.

VALUE:

an object of class `glm` is returned, which inherits from `lm`. See `glm.object` for details.

DETAILS:

The output can be examined by `print`, `summary`, `plot`, and `anova`. Components can be extracted using `predict`, `fitted`, `residuals`, `deviance`, `formula`, and `family`. It can be modified using `update`. It has all the components of an `lm` object, with a few more. Other generic functions that have methods for `glm` objects are `drop1`, `add1`, `step` and `preplot`. Use `glm.object` for further details.

The response variable must conform with the definition of `family`, for example factor or binary data if `family=binomial` is declared.

The model is fit using Iterative Reweighted Least Squares (IRLS). The working response and iterative weights are computed using the functions contained in the `family` object. GLM models can also be fit using the function `gam`. The workhorse of `glm` is the function `glm.fit` which expects an `x` and `y` argument rather than a formula.

REFERENCES:

McCullagh, P. and Nelder, J. A. (1983). *Generalized Linear Models*. Chapman and Hall, London.

EXAMPLES:

```
glm(Count~.,data=solder,family=poisson)
```

```
glm(Kyphosis~poly(Age,2)+(Number>10)*Start, family=binomials)
```

```
glm(ozone^(1/3)~bs(radiation,5)+poly(wind,temperature, degree=2),data=air)
```

C. poly function: Generate a Basis for Polynomial Regression.

USAGE:

```
poly(x, 3)
```

```
poly(x, y, 2)
```

```
poly(...)
```

ARGUMENTS:

...: the arguments to poly can be a comma-separated list of numeric vectors or matrices. If the final argument is atomic, positive, and integer-valued, it is taken to be the degree of the polynomial.

VALUE:

a matrix of orthonormal polynomials is returned. For a single vector argument and a trailing degree argument (first case above), a matrix of orthonormal polynomials of given degree is returned (the constant column is excluded). The orthogonality is with respect to the data. For several arguments (vector, matrix, or both), each of the column vectors is used to generate

orthogonal polynomials of the required degree. The columns will be a subset of the tensor product of the orthogonal polynomials of given degree of each of the individual variables. The matrix has an attribute `degree` that is a vector giving the degree of each column.

When called with a single vector argument, `poly` returns an additional attribute `coefs`. This contains the normalization constants used in constructing the orthogonal polynomials. See the documentation for `poly.raw` for information on how these can be used to construct additional evaluations of the same polynomial basis.

EXAMPLES:

```
glm(Kyphosis~poly(Age,3)+Start,family=binomial)
```

D. s function: Specify a Smoothing Spline Fit in a GAM Formula

USAGE:

```
s(x, df=4, spar=0)
```

ARGUMENTS:

`x`: the univariate predictor, or expression, that evaluates to a numeric vector.

df: the target equivalent degrees of freedom, used as a smoothing parameter. The real smoothing parameter (spar below) is found such that $df = \text{tr}(S) - 1$, where S is the implicit smoother matrix. Values for df should be greater than 1, with 1 implying a linear fit.

spar: can be used as smoothing parameter, with values larger than 0.

VALUE:

the vector x is returned, endowed with a number of attributes. The vector itself is used in the construction of the model matrix, while the attributes are needed for the backfitting algorithms `all.wam` or `s.wam` (weighted additive model). Since smoothing splines reproduces linear fits, the linear part will be efficiently computed with the other parametric linear parts of the model.

DETAILS:

Note that `s` itself does no smoothing; it simply sets things up for `gam`.

EXAMPLES:

```
# fit Start using a smoothing spline with 4 df.
y ~ Age + s(Start, 4)

# fit log(Start) using a smoothing spline with 5 df.
y ~ Age + s(log(Start), df=5)
```

E. `lo` function: Specify a Loess Fit in a GAM Formula.

USAGE:

`lo(..., span=0.5, degree=1)`

ARGUMENTS:

`...`: the unspecified ... can be a comma-separated list of numeric vectors, numeric matrix, or expressions that evaluate to either of these. If it is a list of vectors, they must all have the same length.

`span`: the number of observations in a neighborhood. This is the smoothing parameter for a loess fit.

`degree`: the degree of local polynomial to be fit; can be 1 or 2.

VALUE:

a numeric matrix is returned. The simplest case is when there is a single argument to `lo` and `degree=1`; a one column matrix is returned, consisting of a normalized version of the vector. If `degree=2` in this case, a two-column matrix is returned, consisting of a 2d-degree orthogonal-polynomial basis. Similarly, if there are two arguments, or the single argument is a two-column matrix, either a two-column matrix is returned if `degree=1`, or a five-column matrix consisting of powers and products up to degree 2. Any dimensional argument is allowed, but typically one or two vectors are used in practice. The matrix is endowed with a number of attributes; the matrix itself is used in the construction of the model matrix, while the attributes are needed for the backfitting algorithms `all.wam` or `lo.wam` (weighted additive model). Local-linear curve or surface fits reproduce linear responses, while local-quadratic fits reproduce quadratic curves or surfaces. These parts of the loess fit are computed exactly together with the other parametric linear parts of the model. Note that `lo` itself does no smoothing; it

simply sets things up for gam.

EXAMPLES:

```
y ~ Age + lo(Start, span=.5)
```

```
# fit Start using a loess smooth with a span of 0.5.
```

```
y ~ lo(Age) + lo(Start, Number)
```

```
y ~ lo(Age, 0.5) # the argument name for span is not needed.
```

APPENDIX 6

Tables

Table 3.3 Linear regression results for subject #2

SUB #2			
POSTURE	*PRO+EP	LINEAR	REGRESSION
		(CANONICAL CORRELATION)	
		R1	R2
SITTING	R.1	0.2154	0.3256
	P8.1	0.4213	0.7952
	P18.1	0.5241	0.8965
	R.2	0.5221	0.2315
	P8.2	0.8623	0.6657
	P18.2	0.7568	0.8102
	R.3	0.777	0.8412
	P8.3	0.8697	0.5506
	P18.3	0.7405	0.4259
	R.4		0.5648
	P8.4		0.6353
	P18.4		0.5388
STANDING	R.1	0.2534	0.3547
	P8.1	0.9095	0.8984
	P18.1	0.7318	0.2114
	R.2	0.2548	0.3458
	P8.2	0.4323	0.3548
	P18.2	0.8408	0.68
	R.3	0.8277	0.7668
	P8.3	0.9175	0.5839
	P18.3	0.7966	0.8182
	R.4		0.4577
	P8.4		0.7914
	P18.4		0.5834
SUPINE	R.1	0.3028	0.111
	P8.1	0.6828	0.6691
	P18.1	0.7616	0.7342
	R.2	0.8111	0.6969
	P8.2	0.9781	0.9685
	P18.2	0.6368	0.6628
*EP=ELECTRODE POSITIONS			R=REST
1=ANTERIOR			P8=PACING AT 8BPM
2=LATERAL			P18=PACING AT 18BPM
3=POSTERIOR			R1=RESP1
4=ANTERIOR AND POSTERIOR			R2=RESP2

Table 3.4 Linear regression results for subject #3

SUB #3			
POSTURE	*PRO+EP	LINEAR	REGRESSION
		(CANONICAL CORRELATION)	
		R1	R2
SITTING	R.1	0.4104	0.5
	P8.1	0.6841	0.8509
	P18.1	0.4294	0.7349
	R.2	0.6511	0.3589
	P8.2	0.7076	0.3362
	P18.2	0.4721	0.3056
	R.3	0.9666	0.8998
	P8.3	0.8729	0.5836
	P18.3	0.35	0.3889
	R.4		0.6952
	P8.4		0.5702
	P18.4		0.4824
STANDING	R.1	0.3614	0.2356
	P8.1	0.7289	0.7222
	P18.1	0.585	0.6772
	R.2	0.3311	0.4687
	P8.2	0.646	0.5101
	P18.2	0.4238	0.4972
	R.3	0.9555	0.7398
	P8.3	0.6733	0.75591
	P18.3	0.4263	0.5364
	R.4		0.2356
	P8.4		0.8548
	P18.4		0.6832
SUPINE	R.1	0.5769	0.2896
	P8.1	0.357	0.541
	P18.1	0.6179	0.463
	R.2	0.535	0.7758
	P8.2	0.6135	0.8484
	P18.2	0.4904	0.4246
*EP=ELECTRODE POSITIONS			R=REST
1=ANTERIOR			P8=PACING AT 8BPM
2=LATERAL			P18=PACING AT 18BPM
3=POSTERIOR			R1=RESP1
4=ANTERIOR AND POSTERIOR			R2=RESP2

Table 3.5 Linear regression results for subject #4

SUB #4			
POSTURE	*PRO+EP	LINEAR	REGRESSION
		(CANONICAL CORRELATION)	
		R1	R2
SITTING	R.1	0.6412	0.6255
	P8.1	0.74348	0.7761
	P18.1	0.4385	0.3079
	R.2	0.5377	0.4222
	P8.2	0.7192	0.5408
	P18.2	0.3377	0.1614
	R.3	0.9817	0.7548
	P8.3	0.7658	0.7806
	P18.3	0.938	0.6218
	R.4		0.2314
	P8.4		0.9077
	P18.4		0.6307
STANDING	R.1	0.6635	0.5204
	P8.1	0.8702	0.7163
	P18.1	0.5669	0.675
	R.2	0.5929	0.811
	P8.2	0.7566	0.31
	P18.2	0.361	0.281
	R.3	0.8645	0.9189
	P8.3	0.7422	0.6372
	P18.3	0.3596	0.8802
	R.4		0.3291
	P8.4		0.4461
	P18.4		0.3721
SUPINE	R.1	0.3568	0.625
	P8.1	0.5384	0.6217
	P18.1	0.4975	0.7121
	R.2	0.8444	0.748
	P8.2	0.9353	0.9234
	P18.2	0.4426	0.542
*EP=ELECTRODE POSITIONS			R=REST
1=ANTERIOR			P8=PACING AT 8BPM
2=LATERAL			P18=PACING AT 18BPM
3=POSTERIOR			R1=RESP1
4=ANTERIOR AND POSTERIOR			R2=RESP2

Table 3.6 Linear regression results for subject #5

SUB #5			
POSTURE	*PRO+EP	LINEAR	REGRESSION
		(CANONICAL CORRELATION)	
		R1	R2
SITTING	R.1	0.4102	0.521
	P8.1	0.8273	0.5724
	P18.1	0.5031	0.757
	R.2	0.4589	0.3405
	P8.2	0.6182	0.5103
	P18.2	0.4156	0.3373
	R.3	0.8957	0.7548
	P8.3	0.6776	0.5753
	P18.3	0.4759	0.5031
	R.4		0.4256
	P8.4		0.6996
	P18.4		0.569
STANDING	R.1	0.2145	0.3984
	P8.1	0.8784	0.7654
	P18.1	0.3189	0.6532
	R.2	0.23548	0.441
	P8.2	0.9334	0.6264
	P18.2	0.6732	0.5751
	R.3	0.7548	0.6489
	P8.3	0.8875	0.7524
	P18.3	0.4747	0.7458
	R.4		0.5546
	P8.4		0.2458
	P18.4		0.7507
SUPINE	R.1	0.5689	0.5548
	P8.1	0.4621	0.5053
	P18.1	0.86	0.5893
	R.2	0.8975	0.4587
	P8.2	0.4491	0.6252
	P18.2	0.793	0.885
*EP=ELECTRODE POSITIONS			R=REST
1=ANTERIOR			P8=PACING AT 8BPM
2=LATERAL			P18=PACING AT 18BPM
3=POSTERIOR			R1=RESP1
4=ANTERIOR AND POSTERIOR			R2=RESP2

Table 3.7 Linear regression results for subject #6

SUB #6			
POSTURE	*PRO+EP	LINEAR	REGRESSION
		(CANONICAL CORRELATION)	
		R1	R2
SITTING	R.1	0.3302	0.4506
	P8.1	0.5746	0.7581
	P18.1	0.4136	0.7848
	R.2	0.2106	0.22
	P8.2	0.6901	0.5707
	P18.2	0.5921	0.3411
	R.3	0.8406	0.722
	P8.3	0.7754	0.7492
	P18.3	0.581	0.6981
	R.4		0.4588
	P8.4		0.5411
	P18.4		0.5634
STANDING	R.1	0.2101	0.211
	P8.1	0.7432	0.838
	P18.1	0.3736	0.7154
	R.2	0.4606	0.2546
	P8.2	0.6366	0.8386
	P18.2	0.3533	0.5068
	R.3	0.7891	0.8887
	P8.3	0.6127	0.688
	P18.3	0.6859	0.5836
	R.4		0.1245
	P8.4		0.603
	P18.4		0.8642
SUPINE	R.1	0.4669	0.5505
	P8.1	0.5877	0.6996
	P18.1	0.5421	0.4457
	R.2	0.5896	0.6624
	P8.2	0.8826	0.8306
	P18.2	0.7279	0.6177
*EP=ELECTRODE POSITIONS			R=REST
I=ANTERIOR			P8=PACING AT 8BPM
2=LATERAL			P18=PACING AT 18BPM
3=POSTERIOR			R1=RESP1
4=ANTERIOR AND POSTERIOR			R2=RESP2

Table 3.11 Nonlinear regression results for subject #2

SUB #2				NONLINEAR	REGRESSION		
POSTURE	*PRO+EP			RESIDUAL	DEVIANCE	(GAM)	
		R1(LO)	R1(S)	R1(POLY)	R2(LO)	R2(S)	R2(POLY)
SITTING	R.1	5412.8	4879.99	157891.2	1234.45	3445.08	245005.35
	P8.1	6928.81	44387.49	338768.8	7803.3	23860.25	195541
	P18.1	64548.57	85333.29	1580006.1	47610.23	50803.22	187781.3
	R.2	5889.99	69875.05	453321.12	5488.02	67458.99	10540.5
	P8.2	8894.12	45789.33	457852.88	8523.12	12895.24	179954.2
	P18.2	27714.04	39588.21	88999.89	31913.34	46724.17	113427.1
	R.3	566.44	987.77	145823.02	458.02	5879.99	124570.2
	P8.3	1088.38	4649.91	200107.1	3710.2	12513.5	122091.1
	P18.3	20969.3	22312.38	38191.71	40914.94	62617.85	82419.03
	R.4				54899	65789.03	145898.05
	P8.4				177194.1	373030.8	2009182
	P18.4				455578.2	648289.4	1455271
STANDING	R.1	87999	100025.02	194587.03	2418.22	32881	83458.99
	P8.1	16330.02	24061.86	182840.2	10921.38	25405.48	136554.7
	P18.1	120748	149445.8	312819.1	88048.17	130530	200983.1
	R.2	5889.32	45789.08	88898.19	2145.68	7895.55	125897.04
	P8.2	3878.52	8980	118092.4	3028.54	11314.54	127020.8
	P18.2	68076.4	80878.08	144541.1	130162	158331.7	252951.3
	R.3	897.33	10002.22	145879.05	122.11	4578.02	235688
	P8.3	15888.88	44468.84	308127.4	800.82	1021.2	23495
	P18.3	13034.37	16962.79	51777.53	8154.5	7572.96	21387.3
	R.4				51478.88	612354	457899.02
	P8.4				6728.54	48050.8	378457.3
	P18.4				239325.8	287301.4	409639.2
SUPINE	R.1	56998	65548.88	17452.22	45887	54789.03	254789.02
	P8.1	19355.09	86028.82	433448.5	8123.27	28433.08	354817.1
	P18.1	21938.13	28954.02	63728.53	41278.82	42306.02	114930.6
	R.2	452.33	5890.24	54897.55	4578.03	54788	588924.02
	P8.2	4513.13	9721.98	88911.98	4144.01	9203.17	78420.28
	P18.2	165034	223070.6	332887.3	89258.33	131183.8	221143.2
*EP=ELECTRODE POSITIONS		R=REST					
1=ANTERIOR		P8=PACING AT 8BPM					
2=LATERAL		P18=PACING AT 18BPM					
3=POSTERIOR		R1=RESP1					
4=ANTERIOR AND POSTERIOR		R2=RESP2					

Table 3.12 Nonlinear regression results for subject #3

SUB #3:							
POSTURE	*PRO+EP			NONLINEAR	REGRESSION		
				RESIDUAL	DEVIANCE	(GAM)	
		R1(LO)	R1(S)	R1(POLY)	R2(LO)	R2(S)	R2(POLY)
SITTING	R.1	2445.1	36098	125540.21	25489.99	54887.02	124587.77
	P8.1	4391.89	8802.07	204069.9	13759.61	90735.49	559827.1
	P18.1	628248.1	840997.1	1189512	190815.2	220585.7	375541.9
	R.2	35469.09	45789.022	458023.22	4580.55	5000.21	102045.22
	P8.2	1446.94	15995.62	255697.8	7306.82	170596.8	1868909
	P18.2	88911.13	133439.2	238528.9	40904.93	633577.4	842074.6
	R.3	458.22	5489	124588.33	598.99	6548.22	15469.99
	P8.3	1979.8	16138.19	72447.03	75.36	1391.238	10485.63
	P18.3	42032.04	61582.14	98765.6	7691.83	10110.98	18251.23
	R.4				4577.02	99874	456996.02
	P8.4				1783.95	7311.86	149793.4
	P18.4				24798.99	34854.14	62527.89
STANDING	R.1	5889.33	8897.02	122145.36	2231.01	5444.12	123458
	P8.1	10698.79	71901.04	384742.9	2506.06	25609.63	824417.2
	P18.1	347697.5	526726.3	1388324	143460.2	218803.5	515189.4
	R.2	5478.22	45689.02	224510.88	8897.1	98788.22	187710.2
	P8.2	4738.63	15712.61	195950.1	1208.04	9318.01	161818.9
	P18.2	148121.3	202066	377770.9	109066.9	169478.7	367981.3
	R.3	231.08	455.21	125469.33	566.01	2001.12	54699.05
	P8.3	12565.35	18825.7	629764.1	288.79	837.37	32583.82
	P18.3	67360.91	66941.6	130391.8	12731.02	14353.95	25845.77
	R.4				4578.88	56999	144546.69
	P8.4				1965.81	4238.38	38572.63
	P18.4				1933.3	19331.3	33733.27
SUPINE	R.1	7890.99	88976	223154.55	23889	456998	458021.12
	P8.1	2273.91	9510.6	55010.07	9228.41	17332.37	1137358
	P18.1	18340.51	25973.59	57360.65	39528.97	44264.44	71591.75
	R.2	5489.66	65879.02	456897	2368.22	50044	305489.11
	P8.2	3059.12	3852.46	32551.71	2495.19	2887.31	15950.07
	P18.2	37485.7	43133.32	137794.3	11679.31	15198.7	29808.5
*EP=ELECTRODE POSITIONS		R=REST					
1=ANTERIOR		P8=PACING AT 8BPM					
2=LATERAL		P18=PACING AT 18BPM					
3=POSTERIOR		R1=RESP1					
4=ANTERIOR AND POSTERIOR		R2=RESP2					

Table 3.13 Nonlinear regression results for subject #4

SUB #4				NONLINEAR	REGRESSION		
POSTURE	*PRO+EP			RESIDUAL	DEVIANCE	(GAM)	
		R1(LO)	R1(S)	R1(POLY)	R2(LO)	R2(S)	R2(POLY)
SITTING	R.1	2331.01	5488.89	14578.36	2399.09	5000.22	14588.11
	P8.1	5953.99	13987.9	170950.3	1381.25	3878.21	38224.85
	P18.1	982850.7	925045.2	2983161	78742.32	82843.65	165423.1
	R.2	45879	58889.44	122548.22	14552	24458.78	233548.01
	P8.2	5823.08	5737.82	148982.3	38402.82	27682.38	870421.5
	P18.2	178378.2	190978.9	389578.6	1188452	1417249	213502
	R.3	448.88	5889	238548.88	540.22	45777.22	77895.22
	P8.3	1287.73	2727.45	11648.1	851.74	2589.81	47049.75
	P18.3	4145.08	6078.15	88564.6	18708.88	67083.7	474115.7
	R.4				8799.89	98789.02	124589.8
	P8.4				12884.5	23391.58	67490.5
	P18.4				41691.33	52231.93	192372.1
STANDING	R.1	5478.33	85448	145898.77	4879.32	5489.2	124578.02
	P8.1	24787.31	30559.89	123188.8	12458.63	12207.32	95585.48
	P18.1	8444.03	9883.11	20128.94	18578.47	1974248	73427.1
	R.2	5469.99	6458.02	12548.11	5598.83	6554.45	778941.02
	P8.2	25468.22	414526	124589.55	31584.25	241577.5	84545.22
	P18.2	48370.59	64700.8	139425.8	179090.1	281853.4	489844.8
	R.3	548.88	4001.2	135987.03	458.02	504.44	123589.02
	P8.3	10309.17	39938.92	484901.5	4574.85	9188.59	270237.7
	P18.3	224140.2	352881.2	683432.9	7130.91	10728.53	19898.04
	R.4				55897	98879.09	144588
	P8.4				1905.95	15727.39	108326.4
	P18.4				2435.88	25878	124588.58
SUPINE	R.1	5548.9	8879.68	452138.03	45882	68997.22	554432.01
	P8.1	848.9	1757.8	25439.99	2200.18	2033.18	42570.96
	P18.1	1721.19	2357.94	4708.21	6534.77	7850.2	18071.97
	R.2	4788.02	55789.22	152545.5	2548.33	45778.25	458987.77
	P8.2	2549.5	5427.03	50271.1	3453.47	6317.85	58440.28
	P18.2	122480.3	149619.8	207783.5	47075.48	58197.52	75517.45
*EP=ELECTRODE POSITIONS		R=REST					
1=ANTERIOR		P8=PACING AT 8BPM					
2=LATERAL		P18=PACING AT 18BPM					
3=POSTERIOR		R1=RESP1					
4=ANTERIOR AND POSTERIOR		R2=RESP2					

Table 3.14 Nonlinear regression results for subject #5

SUB #5				NONLINEAR	REGRESSION		
POSTURE	*PRO+EP			RESIDUAL	DEVIANCE	(GAM)	
		R1(LO)	R1(S)	R1(POLY)	R2(LO)	R2(S)	R2(POLY)
SITTING	R.1	45788.12	4522.12	458796.33	3330.12	4566.03	568977.22
	P8.1	4163.52	10148.12	53324.77	15546.4	54912.87	1081345
	P18.1	89183.1	123402.5	291298.4	74131.4	100944.7	244593.7
	R.2	5441.11	65789.33	124588.23	65547	88779.38	132071.8
	P8.2	27138.8	101728.9	1010597	48389.08	372335.3	4483442
	P18.2	2130155	3096451	6215401	2238480	2250831	4008003
	R.3	555.04	45789	123303.21	2214.06	541236	887965.23
	P8.3	7479.5	12450.2	12225	16968.56	60333.78	1130441
	P18.3	408320.9	512490.6	955240.4	34727.22	81409.37	198560.7
	R.4				54789.12	330896	440788.55
	P8.4				4232.51	15877.56	208419
	P18.4				1000845.1	140562.7	201471.4
STANDING	R.1	6441.03	41452.22	45178.99	6504.04	7973.99	76742.25
	P8.1	1229.86	4666.77	42535.27	50458.65	136138.5	592299.1
	P18.1	132071.6	172280	276963.7	149351.9	212301.5	500232.1
	R.2	8996.33	12354.06	244569.99	9987.77	25461.11	98756.321
	P8.2	703.65	3131.55	173463.4	98561.73	198337.6	835752.9
	P18.2	113968.7	148019.6	400720.1	597192.5	719138.9	1221635
	R.3	889.01	66589.21	456912.11	552.88	648.56	12548.7
	P8.3	3452.65	3664.19	156576	23411.12	21741.9	180524.6
	P18.3	164280.2	211950.4	360209.2	11218.05	13661.08	24595.66
	R.4				5055.08	23614.11	224140.2
	P8.4				1647.56	14471.84	960476.9
	P18.4				537356.5	938523	1338451
SUPINE	R.1	22135.6	88790.52	66904.02	44587.22	90991.03	179092.541
	P8.1	266.65	1830.2	23710.2	1141.6	4850.39	33042.37
	P18.1	6566.96	13484.16	28916.79	103766.5	201577.7	348841.1
	R.2	2366.12	254401	125595.23	8860.21	456600.22	655041.11
	P8.2	6206.9	8112.6	62213.22	2278.51	2702.51	51859.61
	P18.2	13955.37	15014.22	23962.02	42220.12	46450.27	105500.9
*EP=ELECTRODE POSITIONS		R=REST					
1=ANTERIOR		P8=PACING AT 8BPM					
2=LATERAL		P18=PACING AT 18BPM					
3=POSTERIOR		R1=RESP1					
4=ANTERIOR AND POSTERIOR		R2=RESP2					

Table 3.15 Nonlinear regression results for subject #6

SUB #6				NONLINEAR	REGRESSION		
POSTURE	*PRO+EP			RESIDUAL	DEVIANCE	(GAM)	
		R1(LO)	R1(S)	R1(POLY)	R2(LO)	R2(S)	R2(POLY)
SITTING	R.1	22504.1	38997.12	778945.12	1125.01	5488.03	45778.98
	P8.1	56434.28	213804.1	944229.3	14202.48	37972.87	308381.2
	P18.1	1307892	1471709	2481098	38583.32	50255.41	151884.2
	R.2	55842.33	88974.01	123405.55	48552.33	652201.01	548922.3
	P8.2	39470.95	80838.22	871238.7	40435.49	93987.13	467881.3
	P18.2	46281.01	97224.13	789962	41113.88	92381.55	328991.4
	R.3	5581.11	21714.41	255078	4432.38	33358.55	328809.1
	P8.3	2441.81	12348.44	105325.7	215.98	1459.14	22802.53
	P18.3	21851.11	29954.49	65510.68	1172603	1400685	1944617
	R.4				23588	55087.12	224708.22
	P8.4				2588.61	23882.33	685271.8
	P18.4				101442.8	111515	172240.5
STANDING	R.1	4577.22	18054.44	98053.35	58778.99	68789.04	548921.22
	P8.1	1514.79	4871.22	98874.8	9550.35	47410.18	237702.4
	P18.1	499770.5	592639.2	1198222	87824.1	90470.62	217445.4
	R.2	2321.12	8898	73214.44	584.12	68541.11	39815.05
	P8.2	18871.81	78828.38	585778.2	18021.45	43901.22	387981
	P18.2	543470.2	557381.7	1085808	95252.94	128899.9	307335.9
	R.3	2001.13	55321.08	34589.99	1055.02	13388.08	178541.44
	P8.3	20802.97	37258.19	479560	9053.81	23391.3	178259.5
	P18.3	395921.2	485187.9	748181.9	37047.18	51242.4	751542
	R.4				14058.88	15889.98	218754.65
	P8.4				53921.28	148383.5	608336.9
	P18.4				121889.1	158977.9	338018.9
SUPINE	R.1	4482.05	5189.98	1081345.12	88144	19652.23	22806.66
	P8.1	5897.25	12548.25	558794.2	9978.38	12548.77	985847
	P18.1	6325.12	55589	488257.33	2345	535501.01	685897.77
	R.2	2202.11	58997.07	808811.55	3399.05	348541.11	458779.02
	P8.2	532.75	1235.4	9043.75	1150.58	1942.43	10090.92
	P18.2	12245.07	18018.54	22842.1	31819.89	53196.61	118798.19
*EP=ELECTRODE POSITIONS		R=REST					
1=ANTERIOR		P8=PACING AT 8BPM					
2=LATERAL		P18=PACING AT 18BPM					
3=POSTERIOR		R1=RESP1					
4=ANTERIOR AND POSTERIOR		R2=RESP2					

REFERENCES

- [1] J. Akanazi, J. Milic-Emili, J. R. Broell, A. I. Hyman, and J. M. Kinney, "Influence of exercise and CO₂ on breathing pattern in normal man." *Journal of Applied Physiology*, 1979, 47: 192-196.
- [2] J. Akanazi, J. Milic-emili, J.R, Broell, A. I. Hyman, and J. M.Kinney, "Effect of respiratory apparatus on breathing pattern." *Journal of Applied Physiology*, 1980, 48: 577-580.
- [3] R. D. Allison, E. L. Holmes, and J. Nyboer, "Volumetric dynamics of respiration as measured by electrical impedance plethysmography." *Journal of Applied Physiology*, 1963, 4:166-173.
- [4] G. V. Anrep, W. Pascaul, and R. Rossler, " Respiratory variation of the heart rate." *Proc. R. Soc. London Ser. B.* ,1936,119:191-230.
- [5] E. Atazler, "Dilektrographie: handbuch der biologischen arbeitsmethoden." *Berlin-Wyten:Urban und Schwarzberg.*, 1935, 5: 1073-1084.
- [6] L. E. Baker, L.A. Geddes, H. E. Hoff,and C. J. Chaput, "Physiological factors underlying transthoracic impedance variations in respiration." *Journal of Applied Physiology*, 1966, 21:1491-1499.
- [7] L. E. Baker, L.A. Geddes, and H. E. Hoff, "Quantitative evaluation of impedance spirometry in man," *Journal of medical electronics*, 1965, 4:73-77.
- [8] J. E. Benjamin, H. Landt, and L. R. Culver, "The body as a volume conductor and its influence on the electrical field of the heart." *American Journal of Medical Sciences*, 1938, 195: 759.
- [9] J. Chambers, and T. Hastie, *Statistical models in S*, California: Wadsworth and Brooks/Cole advanced books and software, Pacific grove,1990.
- [10] M. Clynes, "Respiratory sinus arrythmia: laws derived from computer simulation." *Journal of Applied Physiology* ,1960,15:863-874.
- [11] W. L. Cooley, and L. L. Richard, "A new design for an impedance pneumograph." *Journal of Applied Physiology* ,1968, 25:429-432.
- [12] M. Cremer, "Ueber die registrierung mechanischer vogaenge auf elektrischen wege, speziell nit hilfe des saitengalvanometers und saitenelektrometers." *Munch Med. Wschr*, 1970, 33:1629-1630.

- [13] C. T. M. Davies, and J. M. M. Neilson, "Sinus arrhythmia in man at rest." *Journal of Applied Physiology*, 1967, 22:947-955.
- [14] P. Dejours, R. Pucinelli, J. Armand, and M. Dichary, "Breath-to-breath variations of pulmonary exchange in resting man." *Respiratory Physiology*, 1966, 1:265-280.
- [15] R. C. Elston, and W. D. Johnson, *Essentials of biostatistics*, Philadelphia: F. A. Davis company, 1987.
- [16] C. Fenning, "A new method for recording physiological activities." *I. Lab. Clin. Medicine*, 1936, 22:1279.
- [17] U. Freyschuss, and A. Melcher. "Sinus arrhythmia in man: influence of tidal volume and oesophageal pressure." *Scandinavian Journal of Clinical Laboratory Investigation*, 1966, 36: 487-496.
- [18] U. Freyschuss, and A. Melcher, "Sinus arrhythmia in man: relation to cardiovascular pressures." *Scandinavian Journal of Clinical Laboratory Investigation*. 1976, 36: 221-229.
- [19] L. A. Geddes, H. E. Hoff, D. M. Hickman, M. Hinds, and L. Baker, "The impedance pneumograph." *Aerospace medicine*, 1962, 33:28-33.
- [20] L. A. Geddes, H. E. Hoff, D. M. Hickman, M. Hinds, and L. Baker, "Recording respiration and electrocardiogram with common electrodes." *Aerospace medicine*, 1962, 33:791.
- [21] R. J. Gilbert, J. H. Auchincloss, J. Brodsky, and W. Boden, "Changes in tidal volume, frequency, and ventilation induced by their measurement." *Journal of Applied Physiology*, 1972, 33:252-254.
- [22] P. M. S. Gillam, "Patterns of respiration in human beings at rest and during sleep." *Bulletin of Physiopath Respiration*, 1972, 8:1059-1070.
- [23] H. S. Goldensohn, and L. Zablow, "An electrical impedance spirometer." *Journal of Applied Physiology*, 1959, 14:463-464.
- [24] L. Goodman, "Oscillatory behavior of ventilation in resting man." *IEEE Transactions on Biomedical Engineering*, 1964, 11:82-93.
- [25] A. Grenvik, S. Ballou, E. McGinley, J. E. Millen, W. Cooley, and P. Safar, "Impedance pneumography: comparison between chest impedance changes and respiratory volumes in 11 healthy volunteers." *Chest*, 1972, 62: 439-443.

- [26] P. Grossman, J. Beek, and C. A. Wientjes, "A comparison of three quantification methods for estimation of respiratory sinus arrhythmia." *Psychophysiology*, 1990, 27:703.
- [27] L. H. Hamilton, J. D. Beard, R. C. Carmean, and R. C. Kory, "An electrical impedance ventilometer to quantitate tidal volume and ventilation." *Medical research engineering*. 1967, 6:11-16.
- [28] J. B. Hellman, and R.W. Stacy, "Variation of respiratory sinus arrhythmia with age." *Journal of Applied Physiology*, 1976, 41:734-738.
- [29] J. A. Hirsch, and B. Bishop, "Respiratory sinus arrhythmia in humans: how breathing pattern modulates heart rate." *American Journal of Physiology*, 1981, 241:H620-H628.
- [30] P. G. Katona, and F. Jih, "Respiratory sinus arrhythmia: noninvasive measure of parasympathetic cardiac control." *Journal of Applied Physiology*, 1976, 39:801-805.
- [31] W. Kaufman, and R.D. Johnston, "The electrical conductivity of the tissues near the heart and its bearing on the distribution of cardiac action currents." *American heart Journal*, 1943, 26:42-54.
- [32] J. D. S. Kay, E. Strange Petersen, and H. Vejby-Christensen, "Mean and breath-by-breath pattern of breathing in man during steady-state exercise." *J. Physiol. Lond.* 1975, 251:444-669.
- [33] S. Kira, H. Yasunobi, K. Satoshi, and I. Ayao, "Transthoracic electrical impedance variations associated with respiration." *Journal of Applied Physiology*, 1971, 30:820-826.
- [34] W. G. Kubicek, E. Kinnen, and A. Edin, "Calibration of an impedance pneumograph." *Journal of Applied Physiology*, 1964, 19:557-560.
- [35] Y. Kuratomi, N. Okazaki, T. Ishihara, T. Arai, and S. Kira, "Variability of breath-by-breath volume and its characteristics in normal and diseased subjects: ventilatory monitoring with electrical impedance pneumography." *Japanese Journal of Medicine. Physiology*, 1985, 33:2310-2317.
- [36] H. D. Lauson, R. A. Bloomfield, and A. Cournand, "The influence of respiration on the circulation in man." *American Journal Of Physiology*, 1946, 1:315-336.
- [37] F. Lind, and C. M. Hesser, "Breathing pattern and lung volumes during exercise." *Acta Physiol. Scand.*, 1984, 120:123-129.

- [38] J. L. Logic, M. G. Maksud, and L. H. Hamilton, "Factors affecting transthoracic impedance signals used to measure breathing." *Journal of Applied Physiology*, 1967, 22:251-254.
- [39] C. Lungsgaard, and D. D. Vanslyke, "Studies of lung volume: Relationship between thorax size and lung volume in normal adults." *Journal of experimental medicine*, 1918, 27:65-68.
- [40] J. Mead, and J. L. Whittenberger, "Physical properties of human lungs measured during spontaneous respiration." *Journal of Applied Physiology*, 1953, 5:779.
- [41] J. Mehlsen, K. Pagh, J. S. Neilsen, L. Sestoft, and S. L. Nielsen, "Heart rate response to breathing: dependency upon breathing pattern." *Clinical Physiology*. 1987, 7:115-124.
- [42] A. Melcher, "Respiratory sinus arrhythmia in man." *Acta. Physiol. Scand. Supplementum*, 1976, 535.
- [43] J. Nyboer, "Electrical impedance plethysmography: The electrical resistance measure of the blood pulse volume, peripheral and central blood flow." *Springfiled: Charles . C. Thomas.*, 1951, 66-67.
- [44] D. Paek, and M. F. Dennis, "Breathing patterns during varied activities." *American Journal Of Physiology*, 1992, 1:887:893.
- [45] E. Pasquali, and D. Witsoe, "Problems in impedance pneumography: electrical characteristics of the skin and lung tissues." *Medicine, Biology and engineering*, 1961, 5:249-258.
- [46] S. R. Powers, C. Schaffer, A. Boba, and Y. Nahamura, "Physical and biological factors in impedance plethysmography." *Surgery*, 1958, 44:53.
- [47] J. L. Robotham, W. Lixfeld, L. Holland, D. MacGregor, A. C. Bryan, and J. Rabson, "Effects of respiration on cardiac performance." *Journal of Applied Physiology*, 1978, 44:703-709.
- [48] H. Schaefer, E. Bleicher, and E. Eckervogt, "Weitere beitrage zur elektrischen reizung und zur registrierung von elektrischen vorgargen und der atmung pflug." *Archiv*, 1949, 251: 491.
- [49] A. Selman, A. McDonald, R. Kitney, and D. Linkens, "The interaction between heart rate and respiration: part i - experimental studies in man." *Automedica*, 1982, 4:131-139.

- [50] W. W. Stead, H. S. Wells, N. L. Gault, and J. Ognanovich, "Inaccuracy of the conventional water-filled spirometer for recording rapid breathing." *Journal of Applied Physiology*, 1959, 14:448.
- [51] J. Vander, H. Sherman, and S. Luciano, *Human Physiology - The Mechanisms of body function*, New York: McGraw Hill, 1990.
- [52] O. L. Wade, "Movements of the thoracic cage and diaphragm in respiration." *Journal of Physiology*, 1954, 124:193 .
- [53] G. Weltman, and D. C. Ukkestad, "Impedance pneumograph recording across the arms." *Journal of Applied Physiology*, 1969, 27:907-909.
- [54] J. B. West, "Regional differences in gas exchange in the lung of erect man." *Journal of Applied Physiology*, 1969, 17:893-898.
- [55] J. B. West, *Pulmonary Pathology - The essentials*, Baltimore: Williams and Wilkins, 1987.
- [56] B. F. Womack, "The analysis of respiratory sinus arrhythmia using spectral analysis methods." *IEEE Transactions on Biomedical Engineering*, 1971, 18: 399-409.
- [57] H. Wortel, J. H. Ruiter, G. A. D. Hans, J. P. Heemels, and M. V. Rob, "Impedance measurements in the human right ventricle using a new pacing system." *PACE*, 1991, 14:1336-1342.